Astron. Astrophys. 322, 1–18 (1997)

ASTRONOMY
AND
ASTROPHYSICS

Weak lensing statistics as a probe of Ω and power spectrum

F. Bernardeau[1], **L. Van Waerbeke**[2], **and Y. Mellier**[3,4]
[1]Service de Physique Théorique, C.E. de Saclay, F-91191 Gif-sur-Yvette Cedex, France
[2]Observatoire Midi-Pyrénées, 14 Av. Edouard Belin, F-31400 Toulouse, France
[3]Institut d'Astrophysique de Paris, 98^{bis} Boulevard Arago, F-75014 Paris, France
[4]Observatoire de Paris, (DEMIRM), 61 Av. de l'Observatoire, F-75014 Paris, France

Received 10 October 1996 / Accepted 20 November 1996

Abstract. The possibility of detecting weak lensing effects from deep wide field imaging surveys has opened new means of probing the large-scale structure of the Universe and measuring cosmological parameters. In this paper we present a systematic study of the expected dependence of the low order moments of the filtered *gravitational local convergence* on the power spectrum of the density fluctuations and on the cosmological parameters Ω_0 and Λ. The results show a significant dependence on all these parameters. Though we note that this degeneracy could be partially raised by considering two populations of sources, at different redshifts, computing the third moment is more promising since it is expected, in the quasi-linear regime and for Gaussian initial conditions, to be only Ω_0 dependent (with a slight degeneracy with Λ) when it is correctly expressed in terms of the second moment.

More precisely we show that the variance of the convergence varies approximately as $P(k)\ \Omega_0^{1.5}\ z_s^{1.5}$, whereas the skewness varies as $\Omega_0^{-0.8}\ z_s^{-1.35}$, where $P(k)$ is the projected power spectrum and z_s the redshift of the sources. Thus, used jointly they can provide both $P(k)$ and Ω_0. However, the dependence on the redshift of the sources is large and could be a major concern for a practical implementation.

We have estimated the errors expected for these parameters in a realistic scenario and sketched what would be the observational requirements for doing such measurements. A more detailed study of an observational strategy is left for a second paper.

Key words: cosmology: dark matter; large-scale structures; gravitational lensing

1. Introduction

The detection of weak gravitational lensing effects (weak shear and magnification bias) at large distance from cluster centers is now well established (see Fort & Mellier 1994 and Narayan & Bartelmann 1996 for reviews). With the present development of wide field CCD detectors mounted on the best telescopes it becomes possible to start the investigation of large scale structures from lensing effect observations in an angular area of significant size. The shear and the magnification are expected to be imposed on the background galaxies by the density fluctuations along the line-of-sight. Compared to usual determinations of the density fluctuations in the local universe with galaxy counts (in fact, the light distribution), this approach is extremely attractive since it is directly sensitive to the global mass fluctuations regardless of any biases associated with the light distribution. The detection of weak lensing has thus naturally been suggested as a possible means to measure the power spectrum of the large scale density fluctuations (Blandford et al. 1991).

Theoretical studies done by Blandford et al. (1991), Miralda-Escudé (1991a), Kaiser (1992) and more recently by Villumsen (1996) proposed various approaches and discussed the feasibility of observational strategies for some specific cosmological scenarios. In all cases, they concluded that weak lensing induced by large scale structures is detectable with the present techniques. They claimed that the projected power spectrum should be recovered provided some crucial observational issues, namely the correction of image degradation, are solved. However, even if the observational aspects are certainly the main difficulties in the future, different theoretical problems have not been addressed yet. In particular, the dependence of the physical quantities (such as the convergence, see hereafter) on the cosmological parameters have not been discussed in complete detail. Moreover the errors associated with those quantities for realistic scenarios of large scale structure formation. This paper thus is a theoretical study in which we explore the dependence of a priori physical quantities on the cosmological parameters. We will focus our analysis on the second and third moment of the local filtered convergence at large angular scale, i.e. in a regime where Perturbation Theory results are expected to be valid. We take here advantage of many results that have been obtained in the last few years in this regime, showing that the Perturbation Theory calculations give extremely accurate results for the behavior of the high order moments of the cosmic density at large scale (many papers should be quoted, see Juszkiewicz &

Send offprint requests to: F. Bernardeau; fbernardeau@cea.fr

Bouchet 1995 or Bernardeau 1996b for short review papers on the subject).

Our aim is to present quantitative predictions on the behavior of the moments of the one-point probability distribution function of the local convergence as a function of the matter power spectrum, the cosmological parameters Ω_0 and Λ. As long as one is interested in its second moment in the linear regime, results can easily be extrapolated to other quantities such as the magnification or the distortion (see Sect. 3 for more details on these quantities and their relationships). For the third moment however, the choice of the local convergence (or any other scalar quantity) is crucial. The distortion is intrinsically irrelevant since its third moment, for obvious symmetry reasons, should vanish. The first non-trivial moment would then be its kurtosis, the connected part of the fourth moment, but this is then more intricate to calculate, and also would be more difficult to measure. Other scalar quantities could have been considered, such as the local magnification, but it is not (at the second order) directly proportional to the local density, as it is the case for the convergence. This is why we have preferred this latter quantity.

The paper is structured as follows. In Sect. 2 we present the basic equations, valid for any cosmological model, from which we derive the quantities of interest. In Sect. 3 we explore the dependence of the variance of the convergence on the cosmological parameters. In Sect. 4 we consider third order moments. In the last section we present a study of the expected errors due to the use of a finite sample that are expected to affect the measurements of the second and third moment. The errors have been quantified for a realistic scenario (APM like power spectrum in an Einstein-de Sitter Universe). We eventually propose, in view of the previous results, an adapted strategy to do such observations. Throughout the paper we adopt the convention $H_0 = c = 1$, the physical distances have thus to be multiplied by 3000 for $H_0 = 100\ km/s$/Mpc to be expressed in Mpc.

2. The physical model for the galaxy and mass distributions

The gravitational lensing effects makes intervene both the redshift distributions of the lenses and the sources. In the last section we discuss in more detail the knowledge we have or need to have on the sources, but at this stage we simply describe the redshift distribution of these objects by $n(z)\mathrm{d}z$ with the normalization,

$$\int_0^\infty \mathrm{d}z\, n(z) = 1\ . \tag{1}$$

To illustrate the results we will either assume that the sources are all at the same redshift or are given by a broad distribution. In the latter case we adopt a reasonnable analytic model which reproduces the redshift distributions observed in the faint redshift surveys and those expected from models of galaxy evolution (Charlot & Fall in preparation),

$$n(z)\mathrm{d}z = \frac{8}{\Gamma(9/8)} \left(\frac{z}{z_s}\right)^8 \exp\left[-(z/z_s)^8\right]\ \frac{\mathrm{d}z}{z_s}\,, \tag{2}$$

in which it is assumed that the average redshift of the sources is z_s and that the width of the distribution is about $0.4\ z_s$ (see Fig. 1, thin lines in the upper panel).

We are interested in the lensing effects induced by the large-scale density fluctuations that are assumed to have emerged from Gaussian initial conditions. In the linear regime we thus assume that the local density can be written[1],

$$\delta(\mathbf{x}, z) = \int \frac{\mathrm{d}^3\mathbf{k}}{(2\,\pi)^{3/2}}\ D_+(z)\ \delta(\mathbf{k})\ e^{\mathrm{i}\mathbf{k}\cdot\mathbf{x}} \tag{3}$$

where $D_+(z)$ is the time dependence of the linear growing mode. Note that the function $D_+(z)$ depends on the cosmological parameters as well. It is proportional to the expansion factor only for an Einstein-de Sitter universe. The Fourier transforms of the initial local density contrast, $\delta(\mathbf{k})$, are assumed to form a set of Gaussian variables. In such a case the power spectrum $P(k)$ entirely determines the statistical properties of the initial density field. It is defined by

$$\left\langle \delta(\mathbf{k})\, \delta(\mathbf{k}')\right\rangle = \delta_{\mathrm{Dirac}}(\mathbf{k}+\mathbf{k}')\ P(k). \tag{4}$$

From the observed density fluctuation in the APM galaxy survey it is possible to construct a realistic power spectrum $P(k)$ for both its magnitude and its shape. Using the results of Baugh & Gaztañaga (1996) we can use the shape (we have set $c = H_0 = 1$),

$$P(k) = 1.2\ 10^{-8}\, \frac{k}{\left[1+(k/k_c)^2\right]^{3/2}}, \tag{5}$$

with

$$k_c \approx 150, \tag{6}$$

that reproduces the observed density fluctuations in the *linear* regime[2]. Baugh & Gaztañaga compared the observed fluctuations in the APM galaxy survey with the prediction of this power spectrum and found a good agreement in the linear regime. Results of numerical simulations also show that the nonlinear evolution of the density fluctuations induced with such a spectrum are in good agreement with the observed full shape of the angular two-point correlation function.

In this paper, and contrary to previous studies, we do not make any assumption on both the density of the Universe Ω_0 and on the cosmological constant, Λ.

3. The Weak-Lensing equations

3.1. Description of the deformation in the image plane

The aim of this subsection is to present the mathematical objects that describe the local gravitational deformation. In particular

[1] Note that in case of a non flat Universe, the product $\mathbf{k}\cdot\mathbf{x}$ should be understood as a covariant product, $\mathbf{k}\cdot\mathbf{x} = \chi k_r + \mathscr{D}_0\, k_\perp \cdot \boldsymbol{\xi}$, where $\mathscr{D}_0$ and χ are respectively the angular distance and the distance along the line-of-sight (Sect. 3.3).

[2] We are aware that the adopted power spectrum does not have the expected behaviour, $P(k) \sim k^{-3}$, when $k \to \infty$. But this should not be a problem since we focus our calculations on the linear or quasilinear regime. The large k behaviour of $P(k)$ is therefore not relevant for the purpose of this work.

we recall the relationships between the local convergence κ, the statistical properties of which we will investigate, and the quantities that are more directly observable. We consider two neighboring geodesics $\mathscr{S}$ and $\mathscr{S}'$ which are enclosed by a light bundle, and we call θ_i the two dimensional position angle between $\mathscr{S}$ and $\mathscr{S}'$ at the observer position. Let us define $\boldsymbol{\alpha}$ as the angular diameter distance between $\mathscr{S}$ and $\mathscr{S}'$ at a given redshift z. We assume that the small angle approximation is valid, and we have,

$$\alpha_i(z) = a\, \mathscr{D}_{ij}(z)\, \theta_j, \tag{7}$$

where in the case of an homogeneous Universe, $\mathscr{D}_{ij} = \mathscr{D}_0(z)\delta^K_{ij}$, a being the expansion factor, δ^K_{ij} the Kronecker symbol, and $\mathscr{D}_0(z)$ the physical distance, (see definition hereafter). In an inhomogeneous Universe $\mathscr{D}_{ij}$ describes the deformation of the light bundle produced by the matter distribution. The angular distance $\boldsymbol{\alpha}$ corresponds to an angular position on the sky $\boldsymbol{\xi}$ such that,

$$\boldsymbol{\xi} = \frac{\boldsymbol{\alpha}}{a\,\mathscr{D}_0}\,. \tag{8}$$

The shapes of the light bundles on the image plane are described by the amplification matrix $\mathscr{A}$, the Jacobian of the transformation from a virtual screen located at z (the source plane), to the image plane as seen by the observer. Its inverse, $\mathscr{A}^{-1}$, is actually more closely related to observable quantities,

$$\mathscr{A}^{-1}{}_{ij}(\boldsymbol{\alpha}, z) = \frac{\partial \xi_i}{\partial \theta_j}\,. \tag{9}$$

The amplification matrix can be expressed in terms of the geometrical deformation of the light bundle, the convergence κ and the shear components γ_1 and γ_2 (Schneider et al. 1992),

$$\mathscr{A}^{-1}(\boldsymbol{\xi}) = \begin{pmatrix} 1-\kappa-\gamma_1 & -\gamma_2 \\ -\gamma_2 & 1-\kappa+\gamma_1 \end{pmatrix}. \tag{10}$$

In particular the local convergence $\kappa(\boldsymbol{\xi})$ is given by the trace of this matrix, through the equation,

$$\kappa(\boldsymbol{\xi}) = 1 - \mathrm{tr}\left[\mathscr{A}^{-1}{}_{ij}(\boldsymbol{\xi})\right]/2. \tag{11}$$

The intensity of the shear $\gamma = \gamma_1 + i\gamma_2$ is given by the ratio of the eigenvalues of the matrix $\mathscr{A}^{-1}$. The relations between the physical quantities $(\kappa, \boldsymbol{\gamma})$ and the observable quantities, the magnification (=amplification) μ and the distortion δ of the images, are given by,

$$\mu = \frac{1}{|\mathscr{A}^{-1}|} = \frac{1}{(1-\kappa)^2 - \gamma^2}\;;\quad \boldsymbol{\delta} = \frac{2\boldsymbol{g}}{1+|g|^2}, \tag{12}$$

where $\boldsymbol{g} = \boldsymbol{\gamma}/(1-\kappa)$. Note that in the weak lensing regime we have the simple relations,

$$\mu = 1 + 2\kappa\;;\quad \boldsymbol{\delta} = 2\boldsymbol{\gamma}, \tag{13}$$

In practice, the magnification is measured through the local density of objects (Broadhurst et al. 1995, Broadhurst 1995, Fort et al. 1996) or through the image size of galaxies in different surface brightness slices (Bartelmann & Narayan 1995), whereas the distortion is measured directly from the shape of the background galaxies (Bonnet al. 1994, Fahlman et al. 1994, Smail et al. 1994, Squires et al. 1996a,b). One should be careful when order moments of the local convergence higher than the variance are considered, since non-linear couplings exist in general between μ and $\boldsymbol{\delta}$, and Eqs. (13) cannot be used. It is possible to get the convergence from Eqs. (12) by the measurement of both the magnification and the distortion, or by using only the distortion and the relation introduced by Kaiser (1995, see also Seitz & Schneider 1996) which is valid even beyond the linear regime,

$$\boldsymbol{\nabla}\log(1-\kappa) = \begin{pmatrix} 1+g_1 & g_2 \\ g_2 & 1-g_1 \end{pmatrix}^{-1} \cdot \begin{pmatrix} \dfrac{\partial g_1}{\partial \theta_1} + \dfrac{\partial g_2}{\partial \theta_2} \\ \dfrac{-\partial g_1}{\partial \theta_2} + \dfrac{\partial g_2}{\partial \theta_1} \end{pmatrix}. \tag{14}$$

In the following we will thus assume that the local convergence is accessible to the observations in a given sample, and we will focus our investigations on the statistical properties of this quantity.

3.2. The source equation for the deformation matrix

We perform the calculations assuming that the Born approximation is valid, i.e. that the deformation of a light bundle can be calculated along the unperturbed geodesics. This assumption will be discussed in Sect. 5.7. In a Friedmann-Robertson-Walker (FRW) Universe, such a geodesic may be parameterized by the time variable λ, defined by,

$$\mathrm{d}\lambda = -\frac{\mathrm{d}a}{H(a)},\quad \lambda(a=a_0) = 0, \tag{15}$$

where $H(a)$ is the (time dependent) Hubble constant (in units of H_0). Using the Born approximation and the geodesic deviation equation, the evolution equation for the angular diameter distance $\boldsymbol{\alpha}$ in a lumpy Universe, along the unperturbed ray, as a function of λ is (Seitz 1993),

$$\ddot{\boldsymbol{\alpha}}(\lambda) = \mathscr{R}(\lambda)\boldsymbol{\alpha}(\lambda), \tag{16}$$

where $\mathscr{R}$ is the 2×2 symmetric tidal matrix, and depends on the second derivatives of the Newtonian gravitational potential (Sachs 1961, Seitz 1993),

$$\mathscr{R} = \begin{pmatrix} R - \mathscr{R}e(F) & \mathscr{I}m(F) \\ \mathscr{I}m(F) & R + \mathscr{R}e(F) \end{pmatrix}, \tag{17}$$

$$R = -\frac{1}{2}R_{\alpha\beta}k^\alpha k^\beta\,, \tag{18}$$

$$F = -\frac{1}{2}C_{\alpha\beta\gamma\delta}\epsilon^{\star\alpha}k^\beta\epsilon^{\star\gamma}k^\delta\,, \tag{19}$$

where $R_{\alpha\beta}$ is the Ricci tensor, $C_{\alpha\beta\gamma\delta}$ is the Weyl tensor, k^α is the wave-vector of the light ray and ϵ^α is a complex null vector propagated along the geodesic such that $\epsilon^\alpha k_\alpha = 0$.

Let φ be the 3-dimensional Newtonian gravitational potential. The comoving Poisson equation is,

$$\Delta\varphi = 4\pi G\ \bar{\rho}\ \delta, \tag{20}$$

where $\delta = (\rho - \bar{\rho})/\bar{\rho}$ is the density contrast, Δ is the 3-dimensional Laplacian operator, and the derivatives are done with respect to the proper distance. Note that Eq. (20) does not depend on the cosmological constant Λ. Then, it is straightforward to show that,

$$R = -4\pi G a^{-2}\bar{\rho} - a^{-2}(\partial_{11}\varphi + \partial_{22}\varphi)\ , \tag{21}$$
$$F = -a^{-2}(\partial_{11}\varphi - \partial_{22}\varphi + 2i\partial_{12}\varphi). \tag{22}$$

From Eqs. (7) and (16) the central equation driving the matrix $\mathscr{D}$ is then,

$$\frac{\mathrm{d}^2\left[a(z)\,\mathscr{D}_{ij}(\boldsymbol{\xi},z)\right]}{\mathrm{d}\lambda^2} = a(z)\,\mathscr{R}_{ik}(\boldsymbol{\xi},z)\,\mathscr{D}_{kj}(\boldsymbol{\xi},z), \tag{23}$$

with the boundary conditions,

$$\left(\mathscr{D}_{ij}\right)_{z=0} = 0\ ; \quad \left(\frac{\mathrm{d}\mathscr{D}_{ij}}{\mathrm{d}\lambda}\right)_{z=0} = 1\ . \tag{24}$$

The first equation expresses the focusing condition at the observer, and the second the Euclidean properties of the space at small redshift. $\mathscr{R}_{ij}$ is a symmetric matrix that can be written in terms of φ, and $\bar{\rho}$ using the expressions of R and F,

$$\mathscr{R}_{ij} = -4\pi G\ \bar{\rho}\ a^{-2}\begin{pmatrix}1 & 0\\ 0 & 1\end{pmatrix} - 2a^{-2}\begin{pmatrix}\varphi_{,11} & \varphi_{,12}\\ \varphi_{,21} & \varphi_{,22}\end{pmatrix}. \tag{25}$$

Since $4\pi G\bar{\rho} = 3/2\ \Omega_0/a^3$, for a completely homogeneous universe, the matrix $\mathscr{R}_{ij}$ is given by,

$$\mathscr{R}^{(0)}_{ij} = -\frac{3}{2}(1+z)^5\Omega_0\delta^K_{ij}, \tag{26}$$

and we are left with the equation for the distance

$$\frac{\mathrm{d}^2\left[a(z)\,\mathscr{D}_0(z)\right]}{\mathrm{d}\lambda^2} = -3/2\ (1+z)^4\ \Omega_0\mathscr{D}_0(z). \tag{27}$$

We know that the solution of this differential equation is given by

$$\mathscr{D}_0(z) = \frac{1}{\sqrt{1-\Omega_0-\Lambda}}\ \sinh\left[\sqrt{1-\Omega_0-\Lambda}\int_0^z\frac{\mathrm{d}z'}{E(z')}\right], \tag{28}$$

with

$$E[z] = \sqrt{\Lambda + (1+z)^2\ (1-\Omega_0-\Lambda) + (1+z)^3\ \Omega_0}. \tag{29}$$

This equation has a known analytical solution only when the cosmological constant Λ is zero. Otherwise it has to be integrated numerically.

3.3. The expression of the local convergence

In this section we restrict ourself to the *linear* regime. We then assume that the difference between the local value of $\mathscr{R}_{ij}(\boldsymbol{\xi},z)$ and its value for a homogeneous universe is small, so that,

$$\mathscr{R}^{(1)}_{ij}(\boldsymbol{\xi},z)\ \approx\ \mathscr{R}_{ij}(\boldsymbol{\xi},z) - \mathscr{R}^{(0)}_{ij}(z) \tag{30}$$
$$\equiv\ -\frac{3}{2}\ \Omega_0\ (1+z)^5\ \phi^{(1)}_{,ij}(\boldsymbol{\xi},z), \tag{31}$$

where we have introduced an effective potential ϕ such that,

$$\frac{1}{2}\ \Delta\phi^{(1)}(\boldsymbol{\xi},z) = \delta^{(1)}_{\rm mass}(\boldsymbol{\xi},z) = \frac{\Delta\varphi^{(1)}}{4\pi G\bar{\rho}}, \tag{32}$$

where $\delta^{(1)}_{\rm mass}(\boldsymbol{\xi},z)$ is the local mass over-density in the linear regime. We assume the small angle deviation approximation is valid. In that case, the plane-parallel approximation works, which means that only waves perpendicular to the line-of-sight contribute to lensing, and consequently we can neglect the second order derivative along the unperturbed ray in the Laplacian operator. Moreover, the difference $\mathscr{D}_{ij}(\boldsymbol{\xi},z) - \mathscr{D}_0(z)\ \delta^K_{ij}$ is a small quantity, which can be expanded with respect to the initial density. We then define $\mathscr{D}^{(1)}_{ij}(\boldsymbol{\xi},z)$ as the part of this difference which is linear in this density field (terms of higher order will be considered in Sect. 5). The differential equation for $\mathscr{D}^{(1)}$ can then be derived from (23) and it reads,

$$\frac{\mathrm{d}^2\ \left[a(z)\ \mathscr{D}^{(1)}_{ij}(\boldsymbol{\xi},z)\right]}{\mathrm{d}\lambda^2} - a(z)\,\mathscr{R}^{(0)}_{ik}(z)\,\mathscr{D}^{(1)}_{kj}(\boldsymbol{\xi},z) = -\frac{3}{2}\ \Omega_0\ (1+z)^4\ \mathscr{D}_0(z)\ \phi^{(1)}_{,ij}(\boldsymbol{\xi},z) \tag{33}$$

with

$$(\mathscr{D}^{(1)}_{ij})_{z=0} = 0, \quad \left(\frac{d\mathscr{D}^{(1)}_{ij}}{d\lambda}\right)_{z=0} = 0. \tag{34}$$

To solve this differential equation it is more convenient to write it with the variable z. The differential equation then reads,

$$\frac{\mathrm{d}^2\,\mathscr{D}^{(1)}_{ij}(\boldsymbol{\xi},z)}{\mathrm{d}z^2} + \frac{1}{E(z)}\frac{\mathrm{d}E(z)}{\mathrm{d}z}\ \frac{\mathrm{d}\mathscr{D}^{(1)}_{ij}(\boldsymbol{\xi},z)}{\mathrm{d}z} - \frac{1}{1+z}\ \frac{1}{E(z)}\frac{\mathrm{d}E(z)}{\mathrm{d}z}\ \mathscr{D}^{(1)}_{ij}(\boldsymbol{\xi},z) + \frac{3}{2}\frac{\Omega_0\,(1+z)}{E^2(z)}\ \mathscr{D}^{(1)}_{ij}(\boldsymbol{\xi},z) \tag{35}$$
$$= -\frac{3}{2}\frac{\Omega_0\,(1+z)}{E^2(z)}\ \mathscr{D}_0(\boldsymbol{\xi},z)\,\phi^{(1)}_{,ij}(\boldsymbol{\xi},z). \tag{36}$$

The homogeneous differential equation associated with this equation has two known solutions, the distance functions $\mathscr{D}_0(z)$ and $\mathscr{U}_0(z)$ are given respectively by Eq. (28) and,

$$\mathscr{U}_0(z) = \frac{1}{\sqrt{1-\Omega_0-\Lambda}}\ \cosh\left[\sqrt{1-\Omega_0-\Lambda}\int_0^z\frac{\mathrm{d}z'}{E(z')}\right], \tag{37}$$

from which the solution of the differential equation (33) can be written. Indeed the solution of the inhomogeneous differential

equation reads

$$\mathscr{D}^{(1)}_{ij}(\boldsymbol{\xi},z) = -\frac{3}{2}\,\Omega_0 \int_0^z \mathrm{d}z'\,\frac{(1+z')^4\,\mathscr{D}_0(z')\,\phi^{(1)}_{,ij}(z')}{E^2(z')}\times \frac{\mathscr{U}_0(z)\,\mathscr{D}_0(z') - \mathscr{U}_0(z')\,\mathscr{D}_0(z)}{\mathscr{U}_0'(z')\,\mathscr{D}_0(z') - \mathscr{U}_0(z')\,\mathscr{D}_0'(z')}, \tag{38}$$

which, after elementary mathematical transformations simplifies in,

$$\mathscr{D}^{(1)}_{ij}(\boldsymbol{\xi},z) = -\frac{3}{2}\,\Omega_0 \int_0^z \frac{\mathrm{d}z'}{E(z')}\frac{1}{\sqrt{1-\Omega_0-\Lambda}}\times \sinh\left[\sqrt{1-\Omega_0-\Lambda}\int_{z'}^z \frac{\mathrm{d}\,z''}{E(z'')}\right](1+z')\,\mathscr{D}_0(z')\,\phi^{(1)}_{,ij}. \tag{39}$$

It follows from Eq. (11) that the local convergence can be written for a source at redshift z (see also Seljak 1996),

$$\kappa^{(1)}(\boldsymbol{\xi}) = -\frac{3}{2}\,\Omega_0 \int_0^{\chi(z)} \mathrm{d}\chi(z')\times \frac{\mathscr{D}_0(z',z)\,\mathscr{D}_0(z')}{\mathscr{D}_0(z)}\,(1+z')\,\delta^{(1)}_{\rm mass}(\boldsymbol{\xi},z'), \tag{40}$$

where $\mathscr{D}_0(z',z)$ is the distance between the redshifts z' and z. We have also introduced the new variable $\chi(z)$, very useful for such calculations, which is the physical distance along the line-of-sight,

$$d\chi(z) = \frac{\mathrm{d}z}{E(z)}. \tag{41}$$

It coincides with $\mathscr{D}_0(z)$ only for a flat geometry $\Omega_0+\Lambda=1$. Eq. (40) expresses the fact that the local convergence $\Delta\mu = 2\kappa^{(1)}$ is given by the superposition of the convergence induced by each lens between the observer and the source. For the distribution of sources $n(z)$ we thus have

$$\kappa^{(1)}(\boldsymbol{\xi}) = -\int_0^\infty \frac{\mathrm{d}z'}{E(z')}\,w(z')\delta^{(1)}_{\rm mass}(\boldsymbol{\xi},z'), \tag{42}$$

with

$$w(z') = \frac{3}{2}\,\Omega_0\,(1+z')\,\mathscr{D}_0(z')\int_{z'}^\infty \frac{\mathrm{d}z\,n(z)}{D_0(z)}\times \frac{1}{\sqrt{1-\Omega_0-\Lambda}}\sinh\left[\sqrt{1-\Omega_0-\Lambda}\int_{z'}^z\frac{\mathrm{d}z''}{E(z'')}\right]. \tag{43}$$

The previous two equations are the basic ones that relate the local convergence to the linear cosmic density along the line-of-sight for any cosmological model.

3.4. The efficiency function

We call $w(z)$ in Eq. (43) the efficiency function. It describes the efficiency with which a lens at a given redshift z located along the line-of-sight will affect the local convergence. This efficiency function obviously depends on the redshift of the sources. It is maximum at half the distance between the source and the observer, and vanishes at both ends. In Fig. 1, we present the shape of the efficiency function in different case. In 1a, this is for an Einstein-de Sitter Universe for two different populations of sources. The thin lines show the shape of the distribution functions of the redshifts of the sources that are assumed to be either centered on $z=1$ (solid line) or $z=2$ (dashed line). The typical redshift of the lens is about 0.4 to 0.5, with a broader distribution when the redshift of the sources is larger.

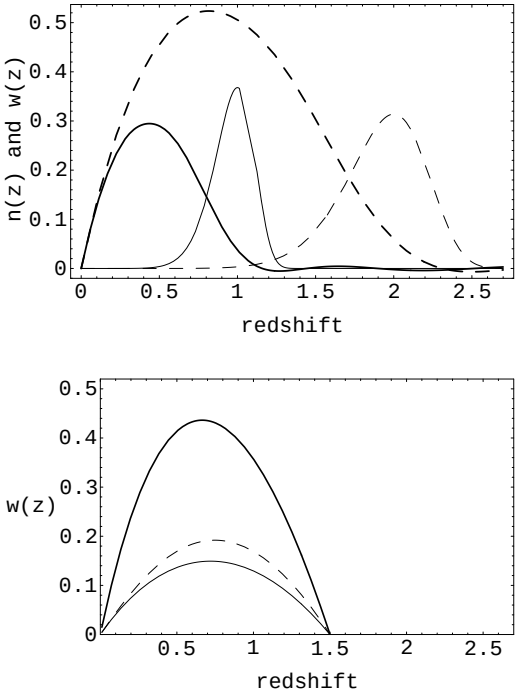

Fig. 1. Shapes of the efficiency functions in different cases. In the upper panel the selection functions $n(z)$ are given by the thin lines (corresponding to Eq. [2] for $z_s = 1$ and z_s=2) and we assume an Einstein-de Sitter Universe. In the lower panel the sources are assumed to be all located at $z_s = 1.5$ and the cosmological parameters are varied, thick solid line for $\Omega = 1$, $\Lambda = 0$, thin solid line for $\Omega = 0.3$ $\Lambda = 0$ and thin dashed line for $\Omega = 0.3$ and $\Lambda = 0.7$.

In the lower panel we show the dependence of the efficiency function on the cosmological parameters. Here the sources are simply assumed to all lie at $z = 1.5$. We can see that the shape of the efficiency function is not really affected. The amplitude is however changed, and it is roughly proportional to Ω_0. The dependence on Λ, although not totally negligible, is considerably weaker than that on Ω_0.

4. The variance of the smoothed convergence

We are interested in the statistical properties of the local convergence at a given scale. We are more particularly interested in the variance at a scale corresponding to the linear or the quasi-linear regime where the interpretation in terms of the cosmological models is easier. For the usual cases, sources at a redshift of about unity, it corresponds to angular scales of about $30'$, or more.

4.1. The convolution with the window function

Throughout this paper we assume that the geometrical filtering is done with a top-hat window function of angular scale θ_0. In the expression (42) the smoothing applies to the $\exp(\mathrm{i}\mathbf{k}\cdot\mathbf{x})$ factor and it gives in the small angle approximation (see Bernardeau 1995),

$$\frac{1}{\pi\,\theta_0^2}\int_0^{\theta_0}\mathrm{d}\theta\int_0^{2\pi}\mathrm{d}\phi\,\exp(\mathrm{i}\mathbf{k}\cdot\mathbf{x}) = \quad (44)$$
$$W_{2D}[k_\perp\mathscr{D}_0(z)\theta_0]\;\exp^{\mathrm{i}\,k_r\chi(z)}.$$

where k_r is the component of $\mathbf{k}$ along the line-of-sight, $k_\perp$ its component in the transverse directions and W_{2D} is the Fourier transform of the 2D top-hat window function,

$$W_{2D}(k) = 2\frac{J_1(k)}{k}, \quad (45)$$

(J_1 is the Bessel function of the first kind). Note that the expression (44) involves both the distance $\mathscr{D}_0(z)$ and the variable $\chi(z)$. These two quantities are identical only for cosmological models with zero curvature.

4.2. The variance in the linear regime

Using the definition (3) of the power spectrum and the relations (44, 42) we get

$$\left\langle\kappa^2(\theta_0)\right\rangle = \frac{1}{2\pi}\int_0^\infty\frac{\mathrm{d}z_1}{E(z_1)}\int_0^\infty\frac{\mathrm{d}z_2}{E(z_2)}\times \quad (46)$$
$$w(z_1)\,w(z_2)\,D_+(z_1)\,D_+(z_2)\int\frac{\mathrm{d}^3\mathbf{k}}{(2\pi)^3}\,P(k)\times$$
$$W_{2D}^2[k_\perp\,D_0(z)\,\theta_0]\;\exp\left[\mathrm{i}\,k_r\,(\chi(z_1)-\chi(z_2))\right].$$

where $D_+(z)$ is the growing mode of the density contrast (cf. Eq. [3]).

We use again the assumption that the deflecting angle and the smoothing angle are small. It implies that

$$P(k)\approx P(k_\perp). \quad (47)$$

Then the integral over k_r yields a Dirac delta function in $\chi(z_1)-\chi(z_2)$ leading to the expression,

$$\left\langle\kappa^2(\theta_0)\right\rangle = \frac{1}{2\,\pi}\int_0^\infty\frac{\mathrm{d}z}{E(z)}\,w(z)^2D_+^2(z)\times$$
$$\int_0^\infty k_\perp\,\mathrm{d}k_\perp\,P(k_\perp)\,W_{2D}^2[k_\perp\,D_0(z)\,\theta_0]. \quad (48)$$

In the following section we explore the properties of this function with different hypotheses for the power spectrum, the redshift distribution of the sources, and the cosmological parameters.

4.3. Realistic results for an Einstein-de Sitter universe

For an Einstein-de Sitter Universe, the distance takes a simple expression as a function of the redshift,

$$\mathscr{D}_0(z) = 2 - 2/\sqrt{1+z} \quad (49)$$

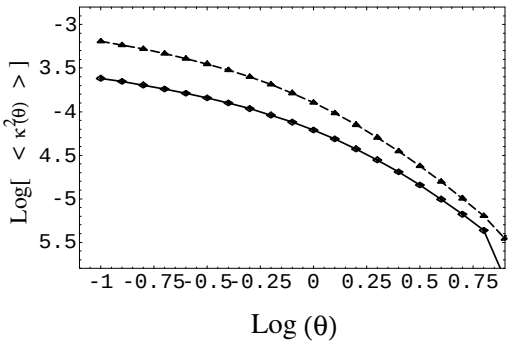

Fig. 2. The expected variance of the convergence as a function of the smoothing angle (in degrees) for $z_s = 1$ (solid line) and $z_s = 2$ (dashed line) in (2) and assuming an Einstein-de Sitter Universe.

and we have,

$$w(z') = \quad \tfrac{3}{2}\,\Omega_0\,(1+z')\,\mathscr{D}_0(z')\;\times$$
$$\int_{z'}^\infty \mathrm{d}z\;n(z)\;\left[1-\mathscr{D}_0(z')/\mathscr{D}_0(z)\right]. \quad (50)$$

We also know that the linear growth rate of the fluctuation is proportional to the expansion factor so that

$$D_+(z) = 1/(1+z). \quad (51)$$

Using the power spectrum given in (5) and the redshift distribution (2) for $z_s = 1$ and $z_s = 2$ we have calculated the angular dependence of the variance of the local smoothed convergence. The results are presented in Fig. 2. We can see that the typical amplitude of the convergence is of the order of a few percent. It starts to bend at an angular scale of about 5 to 10 degrees corresponding to the physical scale where the power spectrum bends down. This scale will be of crucial importance for the evaluation of the cosmic errors on the measured moments.

We can also notice that the results have a significant dependence on the adopted redshift distribution of the sources. In the next subsection we discuss in more detail this point.

4.4. Dependence with the redshift of the sources

We explore here the dependence of the second moment with the redshift of the sources assuming that they are all at a given redshift z_s. We also assume that the power spectrum is given by a power law spectrum. For an Einstein-de Sitter Universe the result reads,

$$\left\langle\kappa^2(\theta_0)\right\rangle \propto \int_0^{\mathscr{D}_0(z_s)}\mathrm{d}\mathscr{D}\,\mathscr{D}^2\,(1-\mathscr{D}/\mathscr{D}_0(z_s))^2\,\mathscr{D}^{-2-n} =$$
$$\frac{2}{(1-n)(2-n)(3-n)}\mathscr{D}_0^{1-n}(z_s) \quad (52)$$

where the angular distance $\mathscr{D}_0$ is given in the Eq. (27). For sources of redshift of the order of 1 or 2, and for a power law index of $n\approx -1.5$, we have approximately,

$$\left\langle\kappa^2(\theta_0)\right\rangle \propto z_s^{1.5}. \quad (53)$$

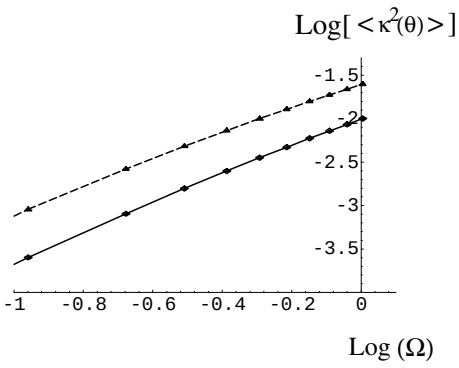

Fig. 3. The expected dependence of the magnitude of the variance on Ω_0 for $z_s = 1$ (solid line) and $z_s = 2$ (dashed line). The overall normalization is arbitrary.

This result confirms the trend observed in the previous subsection. It already indicates that the redshift dependence of the second moment is rather large. Therefore any interpretation of a measurement of such a moment in terms of magnitude of the power spectrum would require a precise knowledge of the sources that have been used. Moreover the magnitude of the second moment depends as well on the values of the cosmological parameters Ω_0 and Λ. The dependence of the results on those parameters is explored in the next subsection.

4.5. Dependence on the cosmological parameters

In this subsection we assume that the power spectrum is a power law and that the sources are all at redshift $z_s = 1$ or $z_s = 2$. In Fig. 3 we then plot the dependence of the second moment on Ω_0 for $\Lambda = 0$. We have approximately

$$\left\langle \kappa^2(\theta_0) \right\rangle \propto \Omega_0^{1.6} \tag{54}$$

for $z_s = 1$ and

$$\left\langle \kappa^2(\theta_0) \right\rangle \propto \Omega_0^{1.4} \tag{55}$$

for $z_s = 2$. The resulting Ω_0 dependence is thus weaker than what one would naively expect from Eq. (48) (e.g. $\left\langle \kappa^2(\theta_0) \right\rangle \propto \Omega_0^2$). The fact that the Ω_0 dependence is actually weaker is mainly due to the growth factor of the linear mode. Indeed at high redshift, for a given normalization at $z = 0$, the lower Ω_0 the larger the density fluctuations are.

In Fig. 4 we present a contour plot of the Ω_0 and Λ dependence of the second moment. We can see that the expected magnitude of the second moment depends essentially on Ω_0. It is however degenerate with Λ when Ω_0 is large. As expected, the Λ dependence is more important when the redshift of the sources is larger.

4.6. The variance with two populations of sources

Interestingly when one considers jointly two different populations of sources, here with $z_s = 1$ and $z_s = 2$, the ratio of the two variances depends on Ω_0 and Λ (see contour plot of Fig. 5) but independent of the normalization of the power spectrum. (The dependence on the power law index is weak).

This is thus, a priori, a way to disentangle the different parameters.

5. Higher-order moments

In this section we explore the possibility of considering higher order moments of the distribution of the local convergence. The idea is that the higher order moments are sensitive to nonlinear aspects of the dynamics and thus could provide independent constraints on the cosmological parameters.

The nonlinear terms in the expression of the fields can be calculated using Perturbation Theory. Similar calculations have been done for the density field and for the local velocity divergence. Comparisons with numerical results have shown that Perturbation Theory calculations give excellent quantitative predictions of the behavior of the high order moments (see Bernardeau 1996b and references therein).

5.1. Second order perturbation theory for the local convergence

The basic assumption of perturbation theory is that the local convergence can be expanded in terms of the initial density field,

$$\kappa(\boldsymbol{\xi}, z) = \kappa^{(1)}(\boldsymbol{\xi}, z) + \kappa^{(2)}(\boldsymbol{\xi}, z) + \dots \tag{56}$$

where $\kappa^{(1)}(\boldsymbol{\xi}, z)$ is linear in the initial density field, so in the variables $\delta(\mathbf{k})$ (this is the term calculated previously), and $\kappa^{(2)}(\boldsymbol{\xi}, z)$ is quadratic in those variables, etc... For calculating the expression of $\kappa^{(2)}(\boldsymbol{\xi}, z)$ we need to use the differential equation (23) up to its second order introducing the expression of

$$\mathscr{R}_{ij}^{(2)}(\boldsymbol{\xi}, z) = -\frac{3}{2}\Omega_0\,(1+z)^5\,\phi_{,ij}^{(2)}(\boldsymbol{\xi}, z) \tag{57}$$

with

$$\frac{1}{2}\Delta\phi^{(2)}(\boldsymbol{\xi}, z) = \delta_{\rm mass}^{(2)}(\boldsymbol{\xi}, z). \tag{58}$$

To find the expression of the local convergence at the second order it is thus necessary to have the expression of the local density at the same order.

The calculation of the second order term for the local density has been investigated in many papers. It has now been calculated for any cosmological model, and a very useful description is given by,

$$\delta_{\rm mass}^{(2)}(\mathbf{x}) = D_+^2(z) \int \mathrm{d}^3\mathbf{k}_1 \mathrm{d}^3\mathbf{k}_2 \delta(\mathbf{k}_1)\delta(\mathbf{k}_2) \times \left(\frac{5}{7} + \frac{\mathbf{k}_1\cdot\mathbf{k}_2}{k_1^2} + \frac{2}{7}\frac{(\mathbf{k}_1\cdot\mathbf{k}_2)^2}{k_1^2 k_2^2} \right) \exp\left[\mathrm{i}\mathbf{x}\cdot(\mathbf{k}_1+\mathbf{k}_2)\right], \tag{59}$$

where the $\delta(\mathbf{k})$ factors are the Fourier transform of the initial density field (cf. [3]).

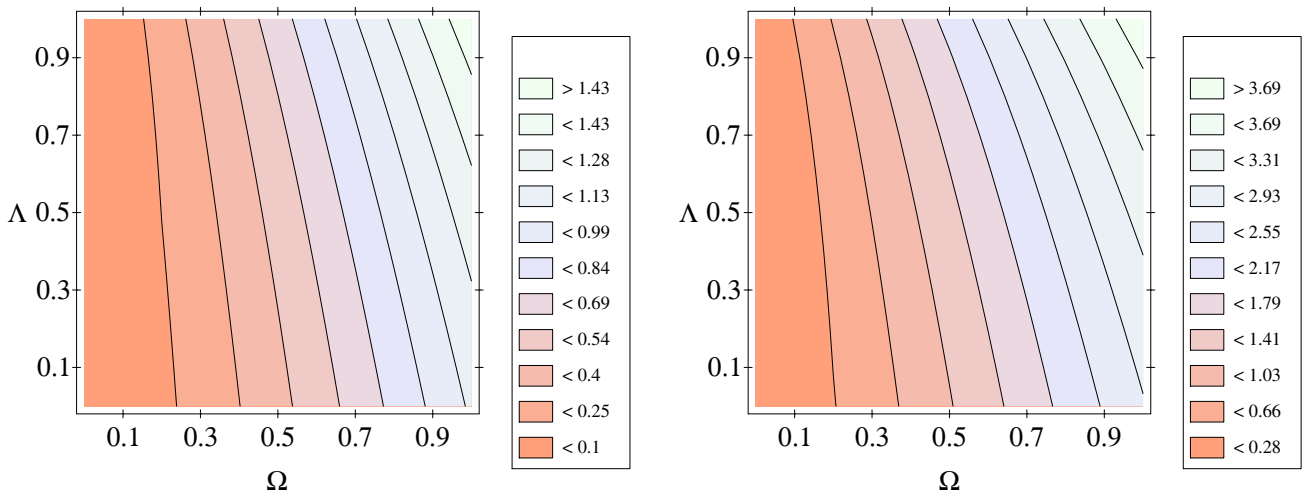

Fig. 4. Contour plots of the expected dependence of the magnitude of the variance on Ω_0 (horizontal axis) and Λ (vertical axis) for $z_s = 1$ (left panel) and $z_s = 2$ (right panel). The lines are iso-values of the variance, normalized to the Einstein-de Sitter case and regularly spaced in linear scale. The variance is stronger at the top right corner of the panels.

The coefficients appearing in this expression given for an Einstein-de Sitter universe, are in fact slightly Ω_0 and Λ dependent (Bouchet et al. 1992, Bernardeau 1994). These dependences are actually so weak (less than 1%) that they can be safely neglected in the subsequent calculations.

The differential equation for $\mathscr{D}^{(2)}_{ij}(\boldsymbol{\xi}, z)$ can be obtained from the Eq. (23), when it is developed up to its second order. We then get,

$$\frac{\mathrm{d}^2\left[a(z)\,\mathscr{D}^{(2)}_{ij}(\boldsymbol{\xi},z)\right]}{\mathrm{d}\lambda^2} - a(z)\,\mathscr{R}^{(0)}_{ik}(z)\,\mathscr{D}^{(2)}_{kj}(\boldsymbol{\xi},z) = -\frac{3}{2}\,\Omega_0\,(1+z)^4\,\phi^{(2)}_{ij}(\boldsymbol{\xi},z)\,\mathscr{D}_0(z) + a(z)\,\mathscr{R}^{(1)}_{ik}(\boldsymbol{\xi},z)\,\mathscr{D}^{(1)}_{kj}(\boldsymbol{\xi},z) \tag{60}$$

with

$$(\mathscr{D}^{(2)}_{ij})_{z=0} = 0\,; \quad \left(\frac{d\mathscr{D}^{(2)}_{ij}}{d\lambda}\right)_{z=0} = 0. \tag{61}$$

The expression of the local convergence can be deduced from the previous two equations,

$$\kappa^{(2)}(\boldsymbol{\xi}) = -\int_0^\infty \frac{\mathrm{d}z'}{E(z')}\,w(z')\times \left[\delta^{(2)}_{\rm mass}(\boldsymbol{\xi},z') - \frac{1}{2}\mathrm{tr}\left[\phi^{(1)}_{ik}(\boldsymbol{\xi},z')\mathscr{D}^{(1)}_{kj}(\boldsymbol{\xi},z')\right]/\mathscr{D}_0(z')\right]. \tag{62}$$

As it can be observed two terms are contributing to this expression. One term is given by the second order density field, the other one is a combination of the linear order of the local density and the linear order in the local amplification. The latter corresponds to the nonlinear coupling introduced by two subsequent deflecting lenses. In the following we will see that the contribution to the third moment is dominated by the first contribution.

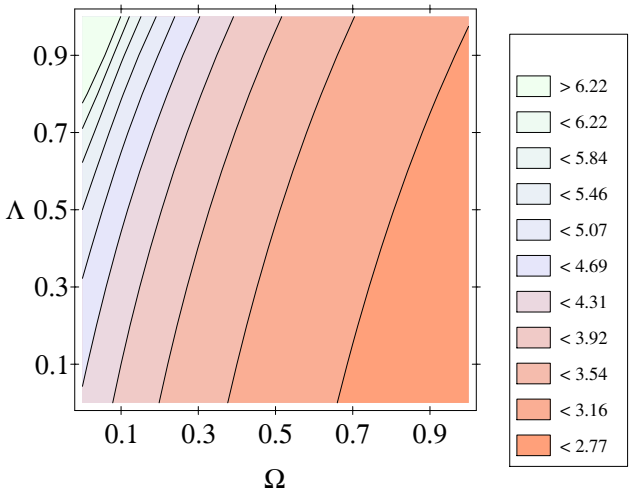

Fig. 5. Contour plot of the expected dependence of the magnitude of the ratio of the two variances on Ω_0 (horizontal axis) and Λ (vertical axis).

5.2. The expression of the local skewness

The principle of such a calculation has been developed in previous papers for the density or the velocity field. It relies on the assumption that the initial density field is Gaussian. As a consequence we have,

$$\left\langle \delta(\mathbf{k}_1)\ldots\delta(\mathbf{k}_{2p+1})\right\rangle = 0 \tag{63}$$

and

$$\left\langle \delta(\mathbf{k}_1)\ldots\delta(\mathbf{k}_{2p})\right\rangle = \sum_{\rm permutations}\prod_{j=1}^{p}\left\langle \delta(\mathbf{k}_{2j-1})\delta(\mathbf{k}_{2j})\right\rangle \tag{64}$$

where the sum over the permutations is made in such a way that all possible pair associations are taken into account.

Then, applying those properties to the initial density field one can calculate the leading term for the expression of the third moment of the local convergence. Using the expansion (56) we have

$$\begin{aligned}\left\langle\kappa^3(\theta_0)\right\rangle &= \left\langle \left(\kappa^{(1)}+\kappa^{(2)}+\ldots\right)^3 \right\rangle \\ &= \left\langle \left(\kappa^{(1)}\right)^3 \right\rangle + 3\left\langle \left(\kappa^{(1)}\right)^2 \kappa^{(2)}\right\rangle + \ldots \end{aligned} \tag{65}$$

The first term of this expression is identically zero in case of Gaussian initial conditions. The dominant contribution to the skewness is thus given by the next-to-leading term, $3\left\langle \left(\kappa^{(1)}\right)^2 \kappa^{(2)}\right\rangle$, that combines both the expression of the linear amplification, and its second order expression.

To compute the previous expression it is worthwhile to know that (Bernardeau 1995)

$$\begin{aligned}&\int \mathrm{d}^2\mathbf{k}_1 \int \mathrm{d}^2\mathbf{k}_2\, W_{2D}\left(|\mathbf{k}_1+\mathbf{k}_2|\right)\, W_{2D}(k_1)\, W_{2D}(k_2)\times \\ &\quad P(k_1)\, P(k_2)\, \left(\frac{5}{7}+\frac{\mathbf{k}_1\cdot\mathbf{k}_2}{k_1^2}+\frac{2}{7}\frac{(\mathbf{k}_1\cdot\mathbf{k}_2)^2}{k_1^2k_2^2}\right) = \\ &\qquad \int \mathrm{d}^2\mathbf{k}_1 \int \mathrm{d}^2\mathbf{k}_2\, P(k_1)\, P(k_2)\times \\ &\left(\frac{6}{7}W_{2D}^2(k_1)W_{2D}^2(k_2)+\frac{1}{4}W_{2D}^2(k_2)\frac{\mathrm{d}W_{2D}^2}{\mathrm{d}k}(k_1)\right).\end{aligned} \tag{66}$$

Using this property we get,

$$\begin{aligned}\left\langle\kappa^3(\theta_0)\right\rangle = \frac{6}{(2\pi)^2}\int_0^\infty \frac{\mathrm{d}z'}{E(z')}\, w(z')^3\, D_+^4(z')\times \\ \left[\frac{6}{7}\left[\int k\mathrm{d}kW_{2D}^2(k)\, P(k)\right]^2 + \right. \\ \left.\frac{1}{2}\int k\,\mathrm{d}k\, W_{2D}^2(k)\, P(k)\times\int k\,\mathrm{d}k\, W_{2D}(k)\, W_{2D}'(k)\, P(k)\right].\end{aligned} \tag{67}$$

This integral can thus be integrated numerically without more technical difficulties than for the second moment[3].

At this stage it is crucial to notice that the ratio,

$$s_3(\theta_0) = \frac{\left\langle\kappa^3(\theta_0)\right\rangle}{\left\langle\kappa^2(\theta_0)\right\rangle^2}, \tag{68}$$

is expected to be *independent of the normalization of the power spectrum*. In the following we will explore in more detail the dependence of this ratio on the different cosmological parameters and physical hypothesis.

To start with let us consider a very simple case in which we assume that we have a power law spectrum, that all sources are at the same redshift z_s and that we live in an Einstein-de Sitter Universe. In such a case we find that

$$\begin{aligned}s_3(z_s) &= -\left[\frac{36}{7}-\frac{3}{2}(n+2)\right]\,(n-1)\,(n-2)\,(n-3)^2\times \\ &\quad \left[40-\frac{4\,n\,(2\,n-1)}{1+z_s}-\frac{32\,n}{\sqrt{1+z_s}}\right]/ \\ &\quad \left[16\,n\,(2\,n-5)\,(2\,n-3)\,(2\,n-1)\,\left(2-2/\sqrt{1+z_s}\right)^2\right] \\ &= -\frac{5535\left(40+\frac{24}{1+z_s}+\frac{48}{\sqrt{1+z_s}}\right)}{32768\left(2-\frac{2}{\sqrt{1+z_s}}\right)^2} \quad \text{for } n=-3/2;\end{aligned} \tag{69}$$

which gives,

$$s_3(z_s) = \approx -42 \quad \text{for } n=-3/2 \ \text{ and } \ z_s=1. \tag{70}$$

This is a quantity a priori accessible to a measurement in a reasonably large catalogue. In the last section we will explore in more detail the expected magnitude of the errors for doing such a measurement. Let us start with a study of the dependence of this quantity on the cosmological parameters.

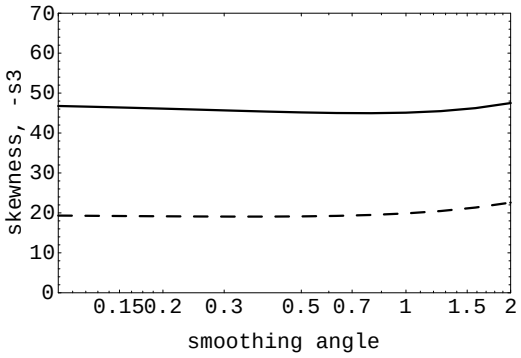

Fig. 6. The expected parameter s_3 as a function of the smoothing angle (in degrees) for $z_s = 1$ (solid line) and $z_s = 2$ (dashed line) in (2), the power spectrum (5) and assuming an Einstein-de Sitter Universe.

5.3. Numerical results for a realistic case

We present in Fig. 6 the results obtained for the function $s_3(\theta_0)$ for the power spectrum (5), the source distribution (2) with z_s = 1 (solid line) and z_s=2 (dashed line) in case of an Einstein-de Sitter Universe. We can see that the function s_3 is rather flat, with little variation with the smoothing angle.

5.4. Dependence on the redshift

From Eq. (69) we easily can visualize the z_s dependence of s_3. This dependence is shown in Fig. 7. We can see that the result is almost independent of the index n, and we have approximately,

$$s_3(z_s) \approx -42\, z_s^{-1.35}. \tag{71}$$

As for the variance, we found that the dependence of the skewness on the redshift of the sources is also quite large.

[3] Note that the property (66) is valid for an angular top-hat window function only, and would not be valid for a Gaussian window function for instance. For other types of window function the dependence of the skewness on the shape of the power spectrum is therefore expected to be more complicated.

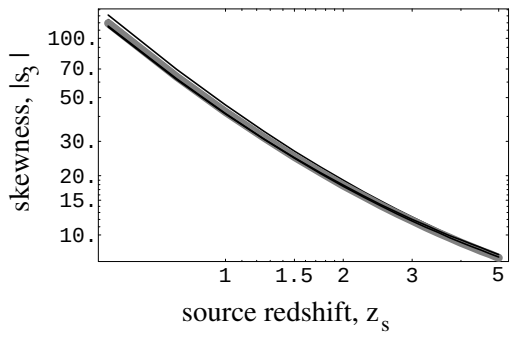

Fig. 7. The expected dependence of s_3 on the redshift of the sources for an Einstein-de Sitter Universe. The curves have been plotted for different power spectrum indices, $n = -1.3,\ -1.5,\ -1.9$ with the thick grey line for the intermediate value

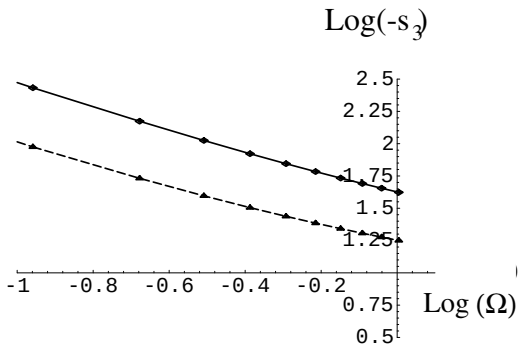

Fig. 8. The expected Ω_0 dependence of s_3 for $z_s = 1$ (solid line) and $z_s = 2$ (dashed line).

5.5. Dependence on the cosmological parameters

From the general formulation we can also explore the dependence of the results on the cosmological parameters. In Fig. 8 we present the Ω_0 dependence of the result for $\Lambda = 0$. We can see that the dependence is rather large, approximatively as

$$s_3(\Omega_0) \approx -42\ \Omega_0^{-0.8} \tag{72}$$

for $z_s \approx 1$. The Ω_0 dependence is actually slightly weaker when the sources are at higher redshift (when the sources are at very small z we recover the natural expectation that s_3 varies inversely with Ω_0.)

In Fig. 9 we then present the contour plot showing the dependence of the parameter on Ω_0 and Λ. We can see that s_3 is significantly less Λ dependent.

5.6. Discussion, simplified model

A this stage it is worth to compare the qualitative results obtained here with those obtained for an a priori similar case: the statistics in an angular survey. In both cases indeed the observed quantities are proportional to the cosmic density integrated along the line-of-sight. The expected properties of the moments of the one-point PDF are however qualitatively different. The reason is that for a 2D angular survey, the density fluctuations are calculated with a selection function implicitly normalized to unity, whereas the efficiency function in the case of the weak lensing is not normalized (see Fig. 1). As a consequence the local convergence is the *summation* of the effects of each lens plane, whereas the local measured galaxy over-density identifies with the *average* of all contributions present on the line-of-sight. The behavior of these quantities is thus dramatically different when the depth of the respective catalogues is changed. The variance of the local convergence increases with the depth (as for a random walk, the mean distance from the center increases as the square root of the number of steps), but it becomes more and more Gaussian, so that s_3 decreases. On the other hand the variance of the local galaxy density contrast decreases with the depth, since the density fluctuations tend to be smoothed out. The parameter s_3 is on the other hand almost independent of this depth. This is exactly what one would obtain by considering respectively the summation or the average of a given number of quasi-Gaussian variables.

From these general remarks one can build a very simple model for the moments of the local convergence that reproduces qualitatively the results discussed in the previous sections. Let us define $\overline{\omega}(z_s)$ as the average of the efficiency function when the sources are at redshift z_s,

$$\overline{\omega}(z_s) = \int_0^{z_s} w(z)\frac{\mathrm{d}z}{E(z)}. \tag{73}$$

Then, from Eqs. (48) and (67) we simply expect that,

$$\left\langle \kappa^2 \right\rangle \propto \frac{\overline{\omega}(z_s)^2}{\mathscr{D}_0^{n+3}(z_s)} \tag{74}$$

$$s_3 \propto \frac{-1}{\overline{\omega}(z_s)}, \tag{75}$$

which show the dependence of these statistical quantities on the efficiency function and the depth of the catalogue. These relations are certainly crude approximations, but explain most of the features encountered previously, such as the dependence of the results on Ω and on the redshift of the sources. It also suggests the existence of a combination of $\left\langle \kappa^2 \right\rangle$ and s_3 that would be almost independent of the redshift of the sources. This combination (which is almost the product of these two quantities, since $\overline{\omega}(z_s)$ is proportional to the distance) would contain information of purely cosmological nature.

5.7. Systematics due to other quadratic couplings

As it can be seen from Eq. (65) the skewness is induced by any quadratic coupling in the observed convergence. In particular it implies that the convergence should not be measured from the local shear using the linear approximation. The method proposed by Kaiser (1995), or a similar method, that takes into account the nonlinear relation between the local shear and the local convergence has to be used.

Spurious couplings can appear also through:

- nonlinear coupling between two deflecting lenses;
- coupling between two deflecting lenses due to the induced displacement of the light path;

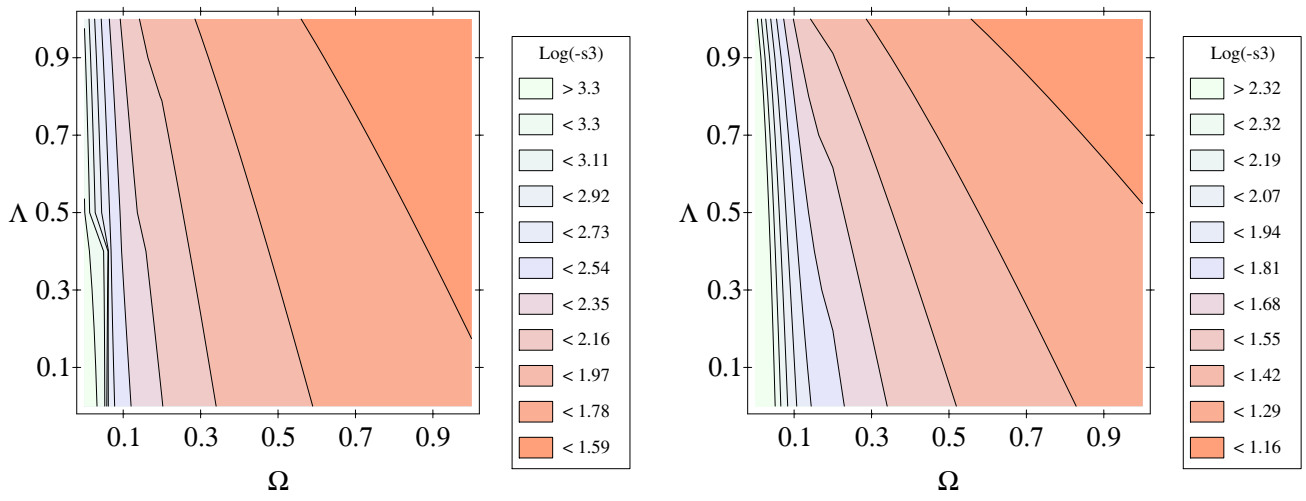

Fig. 9. Contour plot showing the dependence of s_3 on Ω_0 (horizontal axis) and Λ (vertical axis) for $z_s = 1$ (left panel) and $z_s = 2$ (right panel). The contour lines are the logarithmic values of s_3 regularly spaced in a logarithmic scale.

– coupling between the population of selected sources and the local convergence;
– density fluctuations of sources.

In the following we subsequently examine the importance of these different effects.

5.7.1. Coupling between two deflecting lenses

This coupling is due to the fact that when the light path intercepts two lenses the resulting effect is given by the product of the amplification matrices. The resulting convergence $\kappa_{\rm tot}$ is given by the trace of this product, but coincides with the sum of the convergences induced by each lens separately only in the linear regime. In general it is indeed given by

$$\kappa_{\rm tot} = \kappa_A + \kappa_B - \kappa_A\kappa_B - \boldsymbol{\gamma}_A\cdot\boldsymbol{\gamma}_B \tag{76}$$

which contain quadratic terms in the local lens densities (the indices A and B correspond to quantities associated with the lenses A and B respectively).

Actually this nonlinear coupling between two lenses appears in the neglected term in (62). This term induces a corrective expression for the second order convergence term,

$$\kappa^{(2)}_{\rm corr.(1)}(\boldsymbol{\xi}) = \frac{3}{4}\Omega_0\int_0^\infty \frac{{\rm d}z'}{E(z')}\,w(z')\times \tag{77}$$
$$\int_0^{z'}\frac{{\rm d}z''}{E(z'')}\frac{\mathscr{D}_0(z'')\,\mathscr{D}_0(z'',z')}{\mathscr{D}_0(z')}\,\phi^{(1)}_{ik}(\boldsymbol{\xi},z')\,\phi^{(1)}_{ki}(\boldsymbol{\xi},z'').$$

The other source of coupling is due to the failure of the Born approximation (i.e. the densities are calculated along the unperturbed light path) when two lenses are involved. Indeed the convergence induced by a given lens is not due to the local projected density at the observed angular position if a foreground lens shifts the apparent position of the background galaxies. It implies that in (40) the local over-density can be taken at the unperturbed position only at the linear order but in general should be taken at the position $\boldsymbol{\xi}+\delta\boldsymbol{\xi}$ where $\delta\boldsymbol{\xi}$ is the displacement induced by the foreground lenses. To get the quadratic coupling one can simply write,

$$\delta^{(1)}_{\rm mass}(\boldsymbol{\xi}+\delta\boldsymbol{\xi},z) \approx \delta^{(1)}_{\rm mass}(\boldsymbol{\xi},z) + \nabla\delta^{(1)}(\boldsymbol{\xi},z)\cdot\delta\boldsymbol{\xi}. \tag{78}$$

This term induces a term similar to (77),

$$\kappa^{(2)}_{\rm corr.(2)}(\boldsymbol{\xi}) = \frac{3}{4}\Omega_0\int_0^\infty \frac{{\rm d}z'}{E(z')}\,w(z')\times \tag{79}$$
$$\int_0^{z'}\frac{{\rm d}z''}{E(z'')}\frac{\mathscr{D}_0(z'')\,\mathscr{D}_0(z'',z')}{\mathscr{D}_0(z')}\,\phi^{(1)}_{iik}(\boldsymbol{\xi},z')\,\phi^{(1)}_{k}(\boldsymbol{\xi},z'').$$

These two terms obviously induce a corrective term for the skewness. It can be easily calculated, and we estimate it here for an Einstein-de Sitter universe for sources at a fixed redshift z_s. In such a case the second order corrective term for the convergence reads,

$$\kappa^{(2)}_{\rm corr.}(\boldsymbol{\xi}) = \frac{9}{8}\int_0^{\mathscr{D}_0(z_s)}{\rm d}\mathscr{D}'\frac{\mathscr{D}_0(z_s)-\mathscr{D}'}{\mathscr{D}_0(z_s)}\int_0^{\mathscr{D}'}{\rm d}\mathscr{D}''\,\mathscr{D}''\times$$
$$(\mathscr{D}'-\mathscr{D}'')\left[\phi^{(1)}_{ik}(\mathscr{D}')\,\phi^{(1)}_{ki}(\mathscr{D}'')+\phi^{(1)}_{iik}(\mathscr{D}')\,\phi^{(1)}_{k}(\mathscr{D}'')\right] \tag{80}$$

The resulting corrective term for s_3 is

$$s_3^{\rm corr.} = 3\left\langle\kappa^{(2)}_{\rm corr.}\left(\kappa^{(1)}\right)^2\right\rangle/\left\langle\left(\kappa^{(1)}\right)^2\right\rangle^2, \tag{81}$$

so that[4]

$$s_3^{\rm corr.} \approx \frac{\mathscr{D}''}{\mathscr{D}'}\int_0^{\mathscr{D}_0(z_s)}{\rm d}\mathscr{D}'\int_0^{\mathscr{D}'}{\rm d}\mathscr{D}''\left[6-\frac{3}{2}(n+2)\right]\times$$
$$(\mathscr{D}_0(z_s)-\mathscr{D}')^2\,(\mathscr{D}_0(z_s)-\mathscr{D}'')\,(\mathscr{D}'-\mathscr{D}'')\,(\mathscr{D}'')^2\times$$
$$\mathscr{D}'\,\mathscr{D}_0(z_s)\,(\theta_0\,\mathscr{D}')^{-2-n}(\theta_0\,\mathscr{D}'')^{-2-n}/$$
$$\left[\int_0^{\mathscr{D}_0(z_s)}{\rm d}\mathscr{D}'\left(\mathscr{D}'\right)^2(\mathscr{D}_0(z_s)-\mathscr{D}')^2\,(\theta_0\,\mathscr{D}')^{-2-n}\right]^2; \tag{82}$$

$$\approx 1.55 \quad \text{for} \quad n=-3/2, \tag{83}$$

[4] we use here a similar property as in (66), see Bernardeau (1995).

independently of the redshift of the sources. It is completely negligible compared to the main contribution (69), and note that this effect is expected, at first glance, to be mainly independent of Ω_0.

It might be also worth to note that the resulting deformation field induced by two lenses is no more potential (the amplification matrix is not symmetric). As a result, the method proposed by Kaiser (1995) to build the local convergence from the local shear is expected to fail at this level. Once again, this is not expected to be crucial since the effects of this coupling are seen to be small.

5.7.2. Coupling between the population of sources and the convergence

The origin of this effect is the fact that the population of sources on which the shear is measured may change with the local magnification. In this case

$$\kappa^{(2)}_{\rm corr.} = -\kappa^{(1)}(\boldsymbol{\xi}) \int_0^\infty \frac{{\rm d}z'}{E(z')} \frac{\partial w(z')}{\partial \kappa} \delta^{(1)}_{\rm mass}(\boldsymbol{\xi}, z'), \tag{84}$$

with

$$\frac{\partial w(z')}{\partial \kappa} = \frac{3}{2}\,\Omega_0\,(1+z')\,\mathscr{D}_0(z') \int_{z'}^\infty \frac{{\rm d}z}{D_0(z)} \frac{\partial n(z)}{\partial \kappa} \times \frac{1}{\sqrt{1-\Omega_0-\Lambda}}\,\sinh\left[\sqrt{1-\Omega_0-\Lambda}\int_{z'}^z \frac{{\rm d}z''}{E(z'')}\right]. \tag{85}$$

where $\partial n(z)/\partial\kappa$ is the partial derivative of the number density of sources at a given redshift with the local convergence (therefore the local magnification) for a fixed normalization. It can be evaluated a priori from the population of objects used to do the measurements, and on the selection procedure. For instance the mean depth of the sources is expected to change with the local magnification. We can build a simple model in which we assume that the sources are always at a given redshift, but that its corresponding angular distance is a function of the local magnification,

$$\mathscr{D}_0(z_s) = \mathscr{D}^0\,(1+\alpha\,\kappa). \tag{86}$$

It would imply, for an Einstein-de Sitter universe,

$$\frac{\partial w(z)}{\partial \kappa} = \alpha\,\frac{3}{2}\frac{\mathscr{D}_0^2(z)}{\mathscr{D}^0}. \tag{87}$$

In such a case the corrective term for s_3 can be calculated straightforwardly and is given by,

$$s_3^{\rm corr.} = 9\,\alpha\,(1-n)/2, \tag{88}$$

$$\approx 11\,\alpha \ \text{ for } \ n=-1.5. \tag{89}$$

It is not necessarily completely negligible, depending on the value of α, that is the sensitivity of the selected population of sources with the local magnification (this will be explored in more details in the second paper). So, one way to reduce the effect of this coupling is to select the galaxies used to measure the shear from a surface brightness criterion (Bartelmann & Narayan 1995). In practice however, it is probably impossible to suppress all influence in the selection procedure of the total luminosity of the objects.

5.7.3. Coupling due to density fluctuations of sources

Throughout this study we have always implicitly assumed that the sources formed a uniform background population. This is actually far from being true, and one naturally expects the sources to have cosmic density fluctuations. The effects of these fluctuations of the measurements of the local convergences strongly depend on the adopted method. For a method based on the estimation of the local magnification by the depletion of the galaxy number density (magnification bias), this can be a very strong effect on both moments. For methods in which the local convergence is built from the measured shear, this effect is weak. Simple considerations show that it introduces a significant coupling only at the level of the fourth moment. This is due to the fact that the populations of sources and lenses can be considered as two independent populations so there are no direct couplings between their density fluctuations.

6. Error evaluations due to the cosmic variance

In this section we investigate the effects of the cosmic variance on the precision of the measurements of the second moment and on s_3. The origin of this error is the finite size of the sample in which the measurement could be done. Typically we will assume that the sample size is about 25 deg^2, which could be accessible in the coming years for the now available technologies. In this section we describe the measured local convergence, $\kappa_{\rm meas.}(\boldsymbol{\xi})$ as the sum of the exact local convergence and a noise $\epsilon(\boldsymbol{\xi})$,

$$\kappa_{\rm meas.}(\boldsymbol{\xi}_i) = \kappa(\boldsymbol{\xi}_i) + \epsilon(\boldsymbol{\xi}_i). \tag{90}$$

The random noise $\epsilon(\boldsymbol{\xi}_i)$ components are assumed to be all independent of each other, independent of the true values of the local convergence and to have the same variance ϵ,

$$\left\langle \epsilon^2(\boldsymbol{\xi}_i)\right\rangle^{1/2} = \epsilon. \tag{91}$$

It is reasonable to assume that ϵ is of the order of 10^{-3} (see Appendix B). We then introduce the notation $\overline{X}^c$ which is the (connected) geometrical average of the quantity X in the sample. These quantities are also cosmic random variables and are thus expected to vary from one sample to another. Our goal is then to estimate the ensemble averages and variances of those geometrical averages for the quantities of interest, i.e. to know how good they are as estimates of the true cosmic quantities.

To do such calculations we have to introduce the expression of joint moments of the local convergence. Luckily, this is not too complicated! Indeed in the quasi-linear regime one can show that, when the separation between two cells is large compared to the smoothing angle, we have

$$\left\langle \kappa^p(\theta_0,\boldsymbol{\xi}_1)\,\kappa^q(\theta_0,\boldsymbol{\xi}_2)\right\rangle = c_{pq}\,\left\langle \kappa(\theta_0,\boldsymbol{\xi}_1)\,\kappa(\theta_0,\boldsymbol{\xi}_2)\right\rangle\,\left\langle \kappa^2(\theta_0)\right\rangle^{p+q-2}, \tag{92}$$

where c_{pq} are finite quantities. This is the application to 2D statistics of what was developed in 3D by Bernardeau (1996a). However contrary to the 3D case, and due to projection effects, these coefficients depend on the details of the adopted model.

They can anyway be calculated numerically (see Appendix A). Using these results we can calculate both the expectation value of a measured quantity and the variance of this measure. Thus we have

$$\frac{\left\langle\overline{\kappa^2_{\rm meas.}(\theta_0)}\right\rangle - \left\langle\kappa^2(\theta_0)\right\rangle}{\left\langle\kappa^2(\theta_0)\right\rangle} = \frac{\epsilon^2 - \left\langle\kappa^2(\theta_{\rm sample})\right\rangle}{\left\langle\kappa^2(\theta_0)\right\rangle}; \tag{93}$$

$$\frac{\Delta\left\langle\kappa^2_{\rm meas.}(\theta_0)\right\rangle}{\left\langle\kappa^2_{\rm meas.}(\theta_0)\right\rangle} = \sqrt{c_{22}\,\left\langle\kappa^2(\theta_{\rm sample})\right\rangle}; \tag{94}$$

$$\frac{\left\langle s_3^{\rm meas.}\right\rangle - s_3}{s_3} = \left(2 - 3\frac{c_{21}}{s_3}\right)\,\frac{\left\langle\kappa^2(\theta_{\rm sample})\right\rangle}{\left\langle\kappa^2(\theta_0)\right\rangle} - 2\,\frac{\epsilon^2}{\left\langle\kappa^2(\theta_0)\right\rangle}; \tag{95}$$

$$\frac{\Delta s_3^{\rm meas.}}{s_3^{\rm meas.}} = \sqrt{\left(\frac{c_{33}}{s_3^2} + 4c_{22} - 4\frac{c_{32}}{s_3}\right)\,\left\langle\kappa^2(\theta_{\rm sample})\right\rangle}. \tag{96}$$

The numerical calculations give the values of the required coefficients c_{pq} (Appendix A), from which we have

$$\frac{\left\langle\overline{\kappa^2_{\rm meas.}(\theta_0)}\right\rangle - \left\langle\kappa^2(\theta_0)\right\rangle}{\left\langle\kappa^2(\theta_0)\right\rangle} = -0.13; \tag{97}$$

$$\frac{\Delta\left\langle\kappa^2_{\rm meas.}(\theta_0)\right\rangle}{\left\langle\kappa^2_{\rm meas.}(\theta_0)\right\rangle} = 0.14; \tag{98}$$

$$\frac{\left\langle s_3^{\rm meas.} - s_3\right\rangle}{s_3} = -0.07; \tag{99}$$

$$\frac{\Delta s_3^{\rm meas.}}{s_3^{\rm meas.}} = 0.03. \tag{100}$$

The cosmic errors of course decrease with the size of the sample. What the previous results show is that the errors are already quite small when the size of the sample is 25 deg^2 and would allow, for a perfectly well known source distribution, a determination of the cosmological parameters at the 10 to 15% level.

7. Discussion and conclusions

Using Perturbation theory techniques, we have calculated the variance and the skewness of the local filtered convergence κ in an inhomogeneous cosmology in the FRW framework. The quantity κ can be calculated from the measurement of the magnification μ and/or the distortion δ.

The exploration of the dependence of the variance of κ on the parameters of interest have shown that it is, as expected, strongly dependent on Ω_0, but also on Λ. It is of course proportional to the magnitude of the power spectrum of the matter fluctuations. These dependences, although degenerate with each other, are of immediate cosmological interest. Note that these dependences are given for a given power spectrum normalization at redshift zero. As pointed out in other studies (Kaiser 1996, Jain & Seljak in preparation) if the power spectrum is normalized to the present number density of clusters the degeneracy with Ω almost vanishes. More worrying is the fact that the variance is also strongly dependent on the redshift of the sources z_s, making difficult to analyze quantitative results in a cosmological context if the sources are not well known.

It is possible to disentangle the dependence of the variance on the magnitude of the power spectrum and the cosmological parameters by the use of two different populations of sources. Thus, the ratio of the variances for these two populations could provide constraints on the cosmological parameters independently of the power spectrum (the dependence on its shape is only weak). Of course the problem mentioned previously for the knowledge of the population of sources is even more critical since both populations have to be perfectly known.

More interestingly, the skewness s_3 of the local convergence, expressed as the ratio of the third moment and the square of the second, can also provide a way to separate the dependence on the cosmological parameters. We indeed found that this quantity does not depend on the amplitude of the power spectrum, is weakly dependent on its shape and varies almost as the inverse of the density parameter, with a slight degeneracy with the cosmological constant. Moreover the skewness is a probe of the initial Gaussian nature of the density field. If physical mechanisms such as cosmic strings, topological defects, symmetry breaking, etc... generate non Gaussian features in the initial density field, they will modify the behavior of s_3 (see Gaztañaga & Mähönen 1996), inducing a strong angular variation of s_3. The dependence of s_3 on the redshift of the sources is surprisingly large, stressing the absolute necessity of knowing the population of sources used to do such measurements. It is however interesting to note that the product of the variance and the skewness is almost independent of the redshift of sources, so in any case we have a robust estimator of the product $P(k)\ \Omega^{0.5}$. It might reveal to be an interesting quantity to consider.

An important concern was the contribution of multiple lenses configurations in reducing the significance of these statistical estimators. We have shown that the two main quadratic couplings between two lenses are ineffective, with contributions of a few percent, and do not strongly depend on the cosmology. Thus, whatever the cosmological model, the cosmological signal contained in the variance and the skewness could be slightly weakened, but is not washed out by these additional couplings.

We have not considered higher order moments, basically because we think that they are not going to improve the situation, i.e. to raise the degeneracy between the cosmological parameters we have with the second and third moments. A rough calculation (taking into account only the dominant contribution) shows interestingly that the s_4 to s_3^2 ratio is expected to be close to 2 for any cosmological model (Ω_0, Λ and the shape of the power spectrum). In principle it could be used as a test for the gravitational instability scenario with Gaussian initial conditions. We are however far from a reliable measurement of all these quantities.

A concern that has not been addressed in this paper is the validity domain of these results with respect to the nonlinear corrections due to the dynamical evolution of the cosmic fields. These corrections are expected to intervene at small angular scale where the physical scale of the lenses is expected to enter

the nonlinear regime. The question is naturally, at which angular scale? The answer is not straightforward, and actually the situation is slightly different for the second moment and for the skewness. Indeed the second moment is always a measure of the projected power spectrum whether or not it is in the linear regime. This point was clearly made in a recent work (Jain and Seljak, in preparation) where the rms polarization is calculated including the nonlinear evolution of the power spectrum using prescriptions as the ones developed by Hamilton et al. (1991), Jain, Mo & White (1995) and Peacock & Dodds (1996). For s_3 there are no such transformations that would take into account the nonlinear effects. But one should have in mind that this parameter has been observed to be very robust against nonlinear corrections (this is not necessarily the case for the product of the variance and s_3). It has been amply checked in numerical simulations for the 3D filtered density field (see the remarkable results of Baugh, Gaztañaga & Efstathiou, 1995). The situation for the projected density field has not been investigated in as many details, and extended numerical work would be necessary for that respect. In particular it would be interesting to extend the work of Colombi et al. (1996), who propose a prescription to correct the high order moments of the local 3D filtered density PDF, to the projected density. Another arduous line of investigation would be to take into account in the analytic calculations the so called "loop corrections" as it has been pioneered by Scoccimarro & Frieman (1996) for the un-smoothed density field. Such calculations could quantify the errors introduced by the nonlinear effects at small angular scale.

In the last section we have briefly explored the observational requirements for completing a large observational program. We have in particular tried to estimate the cosmic noise that would affect a catalogue covering an area of 25 deg^2. This calculation is at most indicative and should not be considered too realistic. For instance, in this analysis we have made a fairly crude hypothesis for the noise. In particular we have assumed that the noise due to the intrinsic ellipticities of the galaxies is local. If this is true for the local distortion measurement, this is not true for the convergence if it has been obtained from the reconstruction scheme proposed by Kaiser since it involves the gradient of κ. In this analysis we have also not taken into account the fluctuations in the number density of sources, that could be significant at the angular scale we are interested in.

On the other hand we have assumed that the moments were calculated directly, i.e. with the average of the proper power of the different measured convergences. This may not be the most robust way to do it. Indeed, taking advantage of the fact that we expect the Probability Distribution Function of the local convergence to be close to a Gaussian distribution it is possible to estimate the variance and the skewness simply from the shape of the PDF around its maximum. More precisely one can use the Edgeworth expansion (see Juszkiewicz et al. 1995 and Bernardeau & Kofman 1995) to look for the best fitting values of the low order moments without having to actually compute them. With such a method the results should be less sensitive to the cosmic noise, because less sensitive to the rare events in the tails.

We leave for a coming paper the difficult task of defining what we think could be an optimal strategy for observing the shear induced by the large-scale structures and obtaining constraints of cosmological interest out of it. But we stress in any case that such a project demands a lensing survey at 25 square degrees scale with a very high image quality. Such a lensing survey will be used for the statistical work described in this paper, but also to probe the angular power spectrum at scales from the Mpc to few hundred Mpcs. This program is accessible with the UH8K camera or with the future 16K$\times$16K (MEGACAM) camera at the Canada-France-Hawaii Telescope, provided optimal algorithms for measuring very weak shear are used. The pixel to pixel autocorrelation function (ACF) proposed by Van Waerbeke et al. (1996) which consists in analyzing the ellipticity of the ACF induced by the gravitational shear seems a promising approach because it does not require any more to define object centroids and to compute shape parameters for each individual faint galaxy from noisy images. The shape of the sample also impacts on the signal to noise: reconstruction method *à la Kaiser* is expected to introduce finite size errors along the edges of the catalogue, so it would be interesting to have a catalogue as compact as possible. On the other hand an elongated catalogue has less cosmic variance.

The drawback of this project is that it requires the knowledge of the redshift distribution of the sources, especially for faint objects ($B > 25$). A spectroscopic survey to get the redshift of these objects is unrealistic with present-day ground based telescopes; fortunately many other methods are possible, such as the photometric redshifts, the lensing inversion technique, and the depletion method (see Mellier 1996 for a review). None of them have proved their ability to get secure redshifts, but they are potentially very attractive because they are not time consuming.

Acknowledgements. F.B. is grateful to IAP where most of this work has been conducted and to the Observatoire Midi-Pyrénées where it has been completed. The authors are also thankful to the Observatoire de Strasbourg for its very warm hospitality.

Appendix A: expressions of joint cumulants

A.1. General expressions

The statistical quantities described in the main text are expected to be affected by a cosmic variance due to the finite size of the sample. The estimation of such an effect is determined by joint moments between local smoothed convergences taken at two different locations. Indeed these moments provide information on how observed local smoothed convergences are expected to be correlated. The exact derivation of the joint moments of interest would be a difficult task, that requires an explicit calculation of the higher order expression (up to the sixth order!) of the local convergence. As we do not require a very accurate calculation but rather a realistic estimation of these quantities we will make some simplifications in this derivation. First of all we will assume that the high order terms of the local convergence are dominated by the projection along the line-of-sight

of the corresponding high order terms of the local density in the dominant lens plane. This is what has been found in Sect. 5 for the skewness, and we expect it to be also true for the cumulants we are interested in. Moreover to do the calculations we will assume that the size of the sample in which the local convergence is available is significantly larger that the smoothing angular scale. This will make the derivation of the joint cumulants more simple and accessible to Perturbation Theory. Similar results were obtained in a slight different context (Bernardeau 1996a) for which the derivation of joint cumulants is given for 3D top-hat smoothed density contrasts. It is shown that when the distance between the smoothing cells is large compared to the smoothing scale, the joint cumulants can be written,

$$\left\langle \delta_1^p\,\delta_2^q\right\rangle_c \approx\, C_{p,q}\left\langle\delta_1^2\right\rangle^{p-1}\left\langle\delta_2^2\right\rangle^{q-1}\left\langle\delta_1\,\delta_2\right\rangle, \tag{A1}$$

at the leading order in Perturbation Theory, and where the C_{pq} coefficients are finite numbers (they are constant for a power law spectrum). A crucial property for these coefficients is that we have,

$$C_{p,q} = C_{p,1}\,C_{q,1} \tag{A2}$$

so that the derivation of these coefficients reduces to the calculations of a single index series of numbers. They have been given in the paper mentioned above for the 3D top-hat smoothing.

These results cannot be used directly to estimate the joint moments we are interested in, but form however the basis of the calculations. Indeed if we assume, as mentioned in the introduction of this appendix, that the high order expressions of the local convergence are dominated by the projection of the local density of the lenses at the same order, then the expressions of the joint moments are given by the integration over the line-of-sight of the relation (A1) where the coefficients $C_{p,q}$ correspond to the top-hat smoothed joint cumulants *for the 2D dynamics*. This is a situation which is similar to the situation encountered in the derivation of the expression of the high order moments in angular survey.

Using the calculation developed in Bernardeau (1996a) and applying it to the 2D dynamics we get, for a power law spectrum of index n,

$$C_{2,1}^{2D} = \frac{24}{7} - \frac{(n+2)}{2}, \tag{A3}$$

and

$$C_{3,1}^{2D} = \frac{1473}{49} - \frac{195}{14}\,(n+2) + \frac{3}{2}\,(n+2)^2. \tag{A4}$$

Then, as a consequence, the local joint cumulants follow a similar hierarchy

$$\left\langle \kappa(\boldsymbol{\xi}_1)^p\,\kappa(\boldsymbol{\xi}_2)^q\right\rangle_c = \tag{A5}$$
$$c_{p,q}\left\langle\kappa(\boldsymbol{\xi}_1)^2\right\rangle^{p-1}\left\langle\kappa(\boldsymbol{\xi}_2)^2\right\rangle^{q-1}\left\langle\kappa(\boldsymbol{\xi}_1)\,\kappa(\boldsymbol{\xi}_2)\right\rangle,$$

where the coefficients $c_{p,q}$ are given by ratios of integrals along the line-of-sight. We give here the expressions of these integrals for an Einstein-de Sitter Universe, and we will limit the explicit numerical calculations of these expressions for this case,

$$c_{p,q} = C_{p,q}^{2D}\,\frac{Q_{p+q}}{Q_2\,P_2^{p+q-2}}. \tag{A6}$$

with

$$Q_p = \theta_0^{-(n+2)(p-2)} \tag{A7}$$
$$\int_0^{\mathscr{D}_0} \mathrm{d}\mathscr{D}\; w(\mathscr{D})^p\,\mathscr{D}^{(n+2)(p-2)}\,D_+^{2p-2}(\mathscr{D})\,\xi_{2D}(\mathscr{D})$$

$$P_p = \theta_0^{-(n+2)(p-1)} \tag{A8}$$
$$\int_0^{\mathscr{D}_0} \mathrm{d}\mathscr{D}\; w(\mathscr{D})^p\,\mathscr{D}^{(n+2)(p-1)}\,D_+^{2p-2}(\mathscr{D})$$

where

$$\xi_{2D}(\mathscr{D}) = \int_0^\infty k_\perp\,\mathrm{d}k_\perp\,P(k_\perp)\,J_0[k_\perp\,\mathscr{D}\,\theta_{1,2}]. \tag{A9}$$

J_0 is the Bessel function of the first kind and $\theta_{1,2}$ is the angle between the two directions of the smoothing cells 1 and 2.

The final step is to take the geometrical averages of these joint moments in the sample. It is expected to be dominated by cells being at the distance of the order of the size of the sample, $\theta_{\rm sample}$. Then the averaged moments follow the same hierarchy as in (A5) but for which the function $\xi(\mathscr{D})$ is replaced by

$$\bar{\xi}_{2D}(\mathscr{D}) = \int_0^\infty k_\perp\,\mathrm{d}k_\perp\,P(k_\perp)\,W_{2D}^2[k_\perp\,\mathscr{D}\,\theta_{1,2}]. \tag{A10}$$

where W_{2D} is introduced in (45). This result is valid if the sample has a spherical shape, although it is by no means a crucial hypothesis.

In the latter case the integral Q_2 is actually the expression of the variance of the convergence in the whole sample. All the considered joint cumulants are also found to be proportional to this variance, and thus the cosmic uncertainties on the results will be all the more important that this integral is large. The results will therefore depend very strongly on the adopted shape of the power spectrum. In the following subsection we give the numerical results for the APM measured power spectrum (5). Compared to a CDM spectrum it contains more power at large scale and is thus less favorable for the estimation of the cosmic errors, but it is probably more realistic.

A.2. Numerical results

In the following we give the results of the previous integrals for the power spectrum given in (5). The index at the 30' smoothing scale is found to be

$$n \approx -1.45, \tag{A11}$$

and then the coefficients of interest are found to be

$$c_{2,1} = \quad 36.7 \tag{A12}$$
$$c_{2,2} = \quad 1400 \tag{A13}$$
$$c_{3,1} = \quad 3200 \tag{A14}$$
$$c_{3,2} = \quad 125,300 \tag{A15}$$
$$c_{3,3} = 11,400,000 \tag{A16}$$

for a sample size of 25 deg^2, corresponding to a sample size of $\theta_{\rm sample} \approx 3\ deg$. These results are calculated with the distribution of lenses (2) in which $z_s \approx 1$.

Appendix B: evaluation of the cosmic errors

In this appendix we present the derivation of the errors, due to the cosmic variance, i.e. the fact that measurements made in a finite sample are affected by systematic and random errors. We will naturally focus our presentation on the second and third moments of the local smoothed convergence.

To present the calculations it is necessary to introduce two different averages. One is the geometrical average, the mean value of a given observed quantity at different locations, and the second is the ensemble average, which corresponds to the expectation value of quantities that depend on cosmic variables (local densities..) or random quantities associated with intrinsic properties of the galaxies such as their *intrinsic* ellipticities. In principle the two averages of a same quantity coincide in a perfect case, that is if the available data set was infinite, but in practice this is obviously not the case! Actually, the geometrical averages, considered as estimations of the corresponding ensemble averages, are also random variables that are expected to vary from one sample to another. In the following we estimate the properties of these geometrical averages, that is their cosmic expectation values and their variances, assuming that for a sufficiently large sample they obey a Gaussian statistics. We follow here ideas that were developed by Colombi, Bouchet & Schaeffer (1995) and more precisely by Szapudi & Colombi (1996).

B.1. Notations

In the following we denote $\overline{X}^c$ the (connected) geometrical average of a quantity X (and as usual, $\left\langle X \right\rangle_c$ its ensemble average). Thus the observed moments of the measured convergence are

$$\overline{\kappa} = \frac{1}{N_c} \sum_{i=1}^{N_c} \kappa_i \tag{B1}$$

$$\overline{\kappa^2}^c = \frac{1}{N_c} \sum_{i=1}^{N_c} \kappa_i^2 - (\overline{\kappa})^2 \tag{B2}$$

$$\dots$$

where the summations are made over the N_c different locations where the smoothed convergences are supposed to have been determined. We actually assume that the local convergences have been measured in a compact sample, of a size significantly larger than the smoothing length. In the geometrical averages it is also *not* excluded that the smoothing areas overlap, so that N_c can actually be arbitrarily large. Of course the resulting averages cannot be arbitrarily accurate because the measured κ_i are correlated variables, and will be all the more correlated that they are measured in close directions.

B.2. Modelisation

In the following we not only estimate the errors due to the cosmic variance but also the effects of the intrinsic noise in the measurements due to the use of a limited number of tracers for the shear and of their intrinsic imperfections. So assume that the measured convergence in the direction $\boldsymbol{\xi}_i$ is given by,

$$\kappa_{\rm meas.}(\boldsymbol{\xi}_i) = \kappa(\boldsymbol{\xi}_i) + \epsilon(\boldsymbol{\xi}_i), \tag{B3}$$

where $\kappa(\boldsymbol{\xi}_i)$ is the true cosmological value of the local convergence in the direction $\boldsymbol{\xi}_i$ and $\epsilon(\boldsymbol{\xi}_i)$ is the error made in this same direction due to the intrinsic ellipticities of the galaxies. Assuming the ellipticities of the galaxies are independent from one another, and using results obtained for their intrinsic ellipticities (see for instance Miralda-Escudé 1991b) we get,

$$\left\langle \epsilon(\boldsymbol{\xi}_i)^2 \right\rangle \approx \frac{10^{-1}}{\sqrt{n_g}}, \tag{B4}$$

where n_g is the number of galaxies in a given smoothing angular cell. Moreover two variables $\epsilon(\boldsymbol{\xi}_i)$ and $\epsilon(\boldsymbol{\xi}_j)$ are independent if the corresponding cells do not overlap, and they are all assumed to be independent of the true values of the local convergences. This is probably a rather simple and naive modelisation but we leave more accurate numerical studies of a more realistic modelisation for a further paper.

As the variance of $\epsilon(\boldsymbol{\xi}_i)$ is independent of i we will denote, ϵ their common RMS fluctuation,

$$\left\langle \epsilon(\boldsymbol{\xi}_i)^2 \right\rangle = \epsilon^2 \tag{B5}$$

and from the expected density of galaxies in a $(30')^2$ field (about 10^4 for the limit magnitudes $B = 27$ or $I = 26$ currently used in ultra-deep imaging; Tyson 1988, Smail et al. 1995) we can estimate that

$$\epsilon \approx 10^{-3}. \tag{B6}$$

We then define the random variable e_p that describes the departure between an observed geometrical average and the corresponding ensemble average,

$$\overline{\kappa(\theta_0)} = e_1 \tag{B7}$$

and

$$\overline{\kappa^p(\theta_0)}^c = \left\langle \kappa^p(\theta_0) \right\rangle_c (1 + e_p) \tag{B8}$$

for $p > 1$. In the following we will assume that the cosmic random variables e_p have a small variance compared to the variance at the smoothing scale. Therefore the variables e_p can be considered to follow a Gaussian statistics and we will do the calculation at their dominant order. The knowledge of the cosmic errors in any of the considered measurements can then be derived from the values of the variances and cross-correlations between these variables.

B.3. Statistical properties of the variables e_p

To obtain the statistical properties of e_p one can simply consider the ensemble average of the $\overline{\kappa^p(\theta_0)}^c$, of their squares and

products. From the assumed properties of the variables $\epsilon(\boldsymbol{\xi}_i)$ and $\kappa(\boldsymbol{\xi}_i)$ we have,

$$\left\langle \overline{\kappa_{\rm meas.}(\theta_0)} \right\rangle = 0 \tag{B9}$$

$$\left\langle \overline{\kappa_{\rm meas.}(\theta_0)}^2 \right\rangle = \left\langle \kappa^2(\theta_{\rm sample}) \right\rangle \tag{B10}$$

where we have identified the geometrical average of $\left\langle \kappa(\boldsymbol{\xi}_i)\,\kappa(\boldsymbol{\xi}_j) \right\rangle$ with the variance of the local convergence at the scale of the sample, $\theta_{\rm sample}$. At this scale we assume that the ensemble average of $\epsilon(\boldsymbol{\xi}_i)$ is negligible compared to the one of κ: it decreases like Poisson noise, that is more rapidly than the variance of the convergence.

The ensemble averages for the second moment read,

$$\left\langle \overline{\kappa^2_{\rm meas.}(\theta_0)}^c \right\rangle = \left\langle \kappa^2(\theta_0) \right\rangle + \epsilon^2 - \left\langle \kappa^2(\theta_{\rm sample}) \right\rangle \tag{B11}$$

$$\left\langle \left(\overline{\kappa^2_{\rm meas.}(\theta_0)}^c \right)^2 \right\rangle = \left\langle \kappa^2(\theta_0) \right\rangle^2 - 2 \left\langle \kappa^2(\theta_0) \right\rangle \left\langle \kappa^2(\theta_{\rm sample}) \right\rangle + 2\,\epsilon^2 \left\langle \kappa^2(\theta_0) \right\rangle + c_{2,2} \left\langle \kappa^2(\theta_0) \right\rangle^2 \left\langle \kappa^2(\theta_{\rm sample}) \right\rangle \tag{B12}$$

where the calculations have been limited to the quadratic terms in ϵ and $\left\langle \kappa^2(\theta_{\rm sample}) \right\rangle^{1/2}$. The calculations make also intervene the geometrical averages of the joint moments $\left\langle \kappa^2(\boldsymbol{\xi}_i)\,\kappa^2(\boldsymbol{\xi}_j) \right\rangle$ which are evaluated in the previous appendix.

For the third moment we have,

$$\left\langle \overline{\kappa^3_{\rm meas.}(\theta_0)}^c \right\rangle = \left\langle \kappa^3(\theta_0) \right\rangle - 3c_{2,1} \left\langle \kappa^2(\theta_0) \right\rangle \left\langle \kappa^2(\theta_{\rm sample}) \right\rangle, \tag{B13}$$

$$\left\langle \left(\overline{\kappa^3_{\rm meas.}(\theta_0)}^c \right)^2 \right\rangle = \left\langle \kappa^3(\theta_0) \right\rangle^2 + c_{3,3} \left\langle \kappa^2(\theta_0) \right\rangle^4 \left\langle \kappa^2(\theta_{\rm sample}) \right\rangle - 6\,c_{2,1} \left\langle \kappa^2(\theta_0) \right\rangle^3 \left\langle \kappa^2(\theta_{\rm sample}) \right\rangle . \tag{B14}$$

We have also to consider the cross-correlations between those moments which give,

$$\left\langle \overline{\kappa_{\rm meas.}(\theta_0)}^c \, \overline{\kappa^2_{\rm meas.}(\theta_0)}^c \right\rangle = c_{2,1} \left\langle \kappa^2(\theta_0) \right\rangle \left\langle \kappa^2(\theta_{\rm sample}) \right\rangle , \tag{B15}$$

$$\left\langle \overline{\kappa_{\rm meas.}(\theta_0)}^c \, \overline{\kappa^3_{\rm meas.}(\theta_0)}^c \right\rangle = c_{3,1} \left\langle \kappa^2(\theta_0) \right\rangle^2 \left\langle \kappa^2(\theta_{\rm sample}) \right\rangle , \tag{B16}$$

$$\left\langle \overline{\kappa^2_{\rm meas.}(\theta_0)}^c \, \overline{\kappa^3_{\rm meas.}(\theta_0)}^c \right\rangle = \left\langle \kappa^3(\theta_0) \right\rangle^2 - \left\langle \kappa^3(\theta_0) \right\rangle \left\langle \kappa^2(\theta_{\rm sample}) \right\rangle + c_{3,2} \left\langle \kappa^2(\theta_0) \right\rangle^3 \left\langle \kappa^2(\theta_{\rm sample}) \right\rangle - 3\,c_{2,1} \left\langle \kappa^2(\theta_0) \right\rangle^2 \left\langle \kappa^2(\theta_{\rm sample}) \right\rangle + \epsilon^2 \left\langle \kappa^3(\theta_0) \right\rangle. \tag{B17}$$

From these results we have entirely define the statistical properties of the variables e_1, e_2 and e_3. Simple identifications lead to

$$\left\langle e_1 \right\rangle = 0, \tag{B18}$$

$$\left\langle e_1^2 \right\rangle = \left\langle \kappa^2(\theta_{\rm sample}) \right\rangle, \tag{B19}$$

$$\left\langle e_2 \right\rangle = \frac{\epsilon^2 - \left\langle \kappa^2(\theta_{\rm sample}) \right\rangle}{\left\langle \kappa^2(\theta_0) \right\rangle}, \tag{B20}$$

$$\left\langle e_2^2 \right\rangle = c_{2,2} \left\langle \kappa^2(\theta_{\rm sample}) \right\rangle \tag{B21}$$

$$\left\langle e_3 \right\rangle = -3\frac{c_{2,1}}{s_3} \frac{\left\langle \kappa^2(\theta_{\rm sample}) \right\rangle}{\left\langle \kappa^2(\theta_0) \right\rangle}, \tag{B22}$$

$$\left\langle e_3^2 \right\rangle = \frac{c_{3,3}}{s_3^2} \left\langle \kappa^2(\theta_{\rm sample}) \right\rangle, \tag{B23}$$

$$\left\langle e_1 e_2 \right\rangle = c_{2,1} \left\langle \kappa^2(\theta_{\rm sample}) \right\rangle, \tag{B24}$$

$$\left\langle e_1 e_3 \right\rangle = \frac{c_{3,1}}{s_3} \left\langle \kappa^2(\theta_{\rm sample}) \right\rangle, \tag{B25}$$

$$\left\langle e_2 e_3 \right\rangle = \frac{c_{3,2}}{s_3} \left\langle \kappa^2(\theta_{\rm sample}) \right\rangle. \tag{B26}$$

It is interesting to note that ϵ enters only in the expectation value of e_2.

As a result we can calculate both the expectation value of a measured quantity and the variance of this measure. To do so the quantities we are interested in are expressed in terms of the random variables e_p and expanded up to the quadratic order. This is a trivial calculation for the variance, and for the measured s_3 we have

$$s_3^{\rm meas.} = s_3 \frac{1+e_3}{(1+e_2)^2} \approx s_3(1 + e_3 - 2e_2 + 3e_2^2 - 2e_2e_3 + \ldots) \tag{B27}$$

$$\left(s_3^{\rm meas.}\right)^2 = s_3^2 \frac{(1+e_3)^2}{(1+e_2)^4} \approx s_3^2(1 + 2e_3 - 4e_2 + e_3^2 - 8e_2e_3 + 10e_2^2 + \ldots). \tag{B28}$$

Of course this expansion is correct only if the sample size is larger than the smoothing scale.

B.4. Results for the variance and for s_3

Then when we apply the previous rules on the variables e_p and get

$$\frac{\left\langle \overline{\kappa^2_{\rm meas.}(\theta_0)} \right\rangle - \left\langle \kappa^2(\theta_0) \right\rangle}{\left\langle \kappa^2(\theta_0) \right\rangle} = \frac{\epsilon^2 - \left\langle \kappa^2(\theta_{\rm sample}) \right\rangle}{\left\langle \kappa^2(\theta_0) \right\rangle}; \tag{B29}$$

$$\frac{\Delta \left\langle \kappa^2_{\rm meas.}(\theta_0) \right\rangle}{\left\langle \kappa^2_{\rm meas.}(\theta_0) \right\rangle} = \sqrt{c_{22} \left\langle \kappa^2(\theta_{\rm sample}) \right\rangle}; \tag{B30}$$

$$\frac{\left\langle s_3^{\rm meas.} \right\rangle - s_3}{s_3} = \left(2 - 3\frac{c_{21}}{s_3}\right) \frac{\left\langle \kappa^2(\theta_{\rm sample}) \right\rangle}{\left\langle \kappa^2(\theta_0) \right\rangle} - 2\,\frac{\epsilon^2}{\left\langle \kappa^2(\theta_0) \right\rangle}; \tag{B31}$$

$$\frac{\Delta s_3^{\rm meas.}}{s_3^{\rm meas.}} = \sqrt{\left(\frac{c_{33}}{s_3^2} + 4c_{22} - 4\frac{c_{32}}{s_3}\right) \left\langle \kappa^2(\theta_{\rm sample}) \right\rangle}. \tag{B32}$$

One can distinguish two different effects of the cosmic variance for the uncertainties of the results. There is first a systematic shift

proportional to the ratio of the variances. And secondly a cosmic scatter is expected to appear, which is directly proportional to the RMS of the fluctuations of the convergence at the sample scale. It is thus crucial to have a catalogue as large as possible!

Using the numerical results of the previous appendix we have

$$\frac{\left\langle\overline{\kappa^2_{\rm meas.}(\theta_0)}\right\rangle - \left\langle\kappa^2(\theta_0)\right\rangle}{\left\langle\kappa^2(\theta_0)\right\rangle} = -0.13; \tag{B33}$$

$$\frac{\Delta\left\langle\kappa^2_{\rm meas.}(\theta_0)\right\rangle}{\left\langle\kappa^2_{\rm meas.}(\theta_0)\right\rangle} = 0.14; \tag{B34}$$

$$\frac{\left\langle s_3^{\rm meas.}\right\rangle - s_3}{s_3} = -0.07; \tag{B35}$$

$$\frac{\Delta s_3^{\rm meas.}}{s_3^{\rm meas.}} = 0.04. \tag{B36}$$

The cosmic errors of course decreases with the size of the sample. What the previous results show is that the errors are already quite small when the size of the sample is 25 deg^2 and would allow, for a perfectly well known source distribution, a determination of the cosmological parameters at the 5 to 10% level. Note that s_3 appears to be less sensitive to the cosmic variance because it is a ratio of moments.

References

Bartelmann, M., Narayan, R. 1995, ApJ 451, 60.

Baugh, C. & Gaztañaga, E. 1996, MNRAS 280, L37.

Baugh, C.M., Gaztañaga, E. & Efstathiou, G., 1995, MNRAS 274, 1049.

Bernardeau, F. 1994, ApJ 433, 1.

Bernardeau, F. 1995, A&A, 301, 309.

Bernardeau, F. 1996a, A&A, 312, 11.

Bernardeau, F. 1996b, in Proceedings of the XXXI Moriond Meeting "*Dark Matter in Cosmology. Quantum Measurement, Experimental Gravitation*". Les Arcs, France 1996. astro-ph/9607004.

Bernardeau, F. & Kofman, L. 1995, ApJ, 443, 479

Blandford, R. D., Saust, A. B., Brainerd, T. G., Villumsen, J. V. 1991, MNRAS 251, 600.

Bonnet, H., Mellier, Y., Fort, B. 1994 ApJ 427, L83.

Bouchet, F., Juszkiewicz, R., Colombi, S. & Pellat, R. 1992, ApJ, 394, L5

Broadhurst, T. 1995, astro-ph/9511150.

Broadhurst, T., Taylor, A.N., Peacock, J. 1995 ApJ 438, 49.

Charlot, S., Fall, S. M., in preparation

Colombi, S., Bouchet, F. & Schaeffer, R., 1995, ApJS, 96, 401

Colombi, S., Bernardeau, F., Bouchet F. & Hernquist, L., 1996, astro-ph/9610253

Fahlman, G., Kaiser, N., Squires, G., Woods, D. 1994, ApJ 437, 56.

Fort, B., Mellier, Y. 1994, A&AR 5, 239.

Fort, B., Mellier, Y., Dantel-Fort, M. 1996, astro-ph/9606039.

Gaztañaga, E. & Mähönen P. 1996, ApJ, 462, 1.

Hamilton, A.J.S., Kumar, P., Lu, E. & Matthews, A. 1991, ApJ, 374, L1

Jain, B., Seljak, U., in preparation

Jain, B., Mo, H.J., White, S.D.M. 1995, MNRAS, 276, L25

Juszkiewicz, R., Weinberg, D., Amsterdamsky, P., Chodorowski, M. & Bouchet, F. 1995, ApJ, 442, 39

Juszkiewicz, R. & Bouchet, F., 1995, in Proceedings of the XXX Moriond Meeting "*Clustering in the Universe* ". Les Arcs, France 1995.

Kaiser, N. 1992, ApJ 388, L72.

Kaiser, N. 1995, ApJ 439, 1.

Kaiser, N. 1996, astro-ph/9610120

Mellier, Y. 1996, Proceedings of the 37^{th} Herstmonceux Conference "*HST and the High Redshift Universe*". Cambridge 1996. N. Tanvir, A. Aragón-Salamanca, J. V. Wall eds. Preprint astro-ph/9608158.

Miralda-Escudé, J. 1991b, ApJ 370, 1.

Miralda-Escudé, J. 1991a, ApJ 380, 1.

Narayan, R., Bartelmann, M. 1996, astro-ph/9606001.

Peacock, J.A. & S.J. Dodds, 1996, MNRAS 280, L19.

Sachs, R. K. 1961, Proc. Roy. Soc. London A264, 309.

Schneider, P., Ehlers, J., Falco, E. E. 1992, *Gravitational Lenses*, Springer.

Scoccimarro, R. & Frieman, J. 1996, ApJS, 105, 37.

Seitz, S. 1993, Proceeding of the Conference on "*Gravitational Lenses in the Universe*" Liège 1993.

Seitz, S. & Schneider, P. 1996, ApJ, 305, 383.

Seljak, U. 1996, ApJ 463, 1.

Smail, I., Ellis, R.S., Fitchett, M. 1994 MNRAS, 270, 245.

Smail, I., Hogg, D., Yan, L. Cohen, J. G. 1995, ApJ 449, L105.

Squires, G., Kaiser, N., Babul, A., Fahlmann, G., Woods, D., Neumann, D.M., Böhringer, H. 1996a, ApJ, 461, 572.

Squires, G., Kaiser, N., Falhman, G., Babul, A., Woods, D. 1996b, ApJ, 469, 73.

Szapudi, I., Colombi, S., 1996, ApJ, 470, 131

Tyson, J. A. 1988, AJ 96, 1.

Van Waerbeke, L., Mellier, Y., Schneider, P., Fort, B., Mathez, G. 1996, A&A in press, astro-ph/9604137.

Villumsen, J. V. 1996, MNRAS 281, 369.

This article was processed by the author using Springer-Verlag LaTeX A&A style file *L-AA* version 3.